

1 **Genome-wide neighbor effects predict genotype pairs 2 that reduce herbivory in mixed planting**

3 **Yasuhiro Sato^{1,2*}, Rie Shimizu-Inatsugi¹, Kazuya Takeda², Bernhard Schmid³,
4 Atsushi J. Nagano^{4,5*}, Kentaro K. Shimizu^{1,6*}**

5 ¹ Department of Evolutionary Biology and Environmental Studies, University of Zurich,
6 Winterthurerstrasse 190, 8057 Zurich, Switzerland

7 ² Research Institute for Food and Agriculture, Ryukoku University, Yokotani 1-5, Seta
8 Oe-cho, Otsu, Shiga 520-2194, Japan

9 ³ Department of Geography, University of Zurich, Winterthurerstrasse 190, 8057 Zurich,
10 Switzerland

11 ⁴ Faculty of Agriculture Ryukoku University, Yokotani 1-5, Seta Oe-cho, Otsu, Shiga 520-
12 2194, Japan

13 ⁵ Institute for Advanced Biosciences, Keio University, 403-1 Nipponkoku, Daihouji,
14 Tsuruoka, Yamagata, 997-0017, Japan

15 ⁶ Kihara Institute for Biological Research, Yokohama City University, Maioka 641-12,
16 Totsuka-ward, Yokohama 244-0813, Japan

17 *Co-corresponding authors: yasuhiro.sato@uzh.ch (Y.S.); anagano@agr.ryukoku.ac.jp
18 (A.J.N); kentaro.shimizu@uzh.ch (K.K.S.)

19 **Keywords:** Associational resistance, Genetic diversity, Plant-herbivore interaction

20 **Summary**

21 Genetically diverse populations can increase plant resistance to natural enemies. Yet,
22 beneficial genotype pairs remain elusive due to the occurrence of both positive and
23 negative effects of mixed planting on plant resistance, called associational resistance
24 and susceptibility. We used genome-wide polymorphisms of the plant species
25 *Arabidopsis thaliana* to identify genotype pairs that enhance associational resistance to
26 herbivory. By quantifying neighbor interactions among 199 genotypes grown in a
27 randomized block design, we predicted that 823 of the 19,701 candidate pairs could
28 reduce herbivory through associational resistance. We planted such pairs with
29 predicted associational resistance in mixtures and monocultures and found a significant
30 reduction in herbivore damage in the mixtures. Our study highlights the potential
31 application to assemble genotype mixtures with positive biodiversity effects.

32

33 Main Text

34 Genetic diversity is increasingly recognized as a critical facet of biodiversity (1, 2) that
35 should be conserved as a provider of various ecosystem services (3) as well as a source
36 of evolution (2, 4). In terrestrial ecosystems, for example, plant genotypic diversity can
37 increase plant resistance to natural enemies as the number of plant genotypes in a
38 contiguous group of plants, namely a stand, increases (5–7). However, such a stand of
39 multiple plant genotypes does not always result in positive outcomes (8–10).

40 Identifying beneficial pairs from a mixture of genotypes helps us design a desirable
41 mixture and understand the potential mechanisms affecting stand-level properties.

42 Both positive and negative effects of mixed planting on stand-level resistance to
43 herbivores have been reported in the literature (7, 11–13). The underlying mechanisms
44 have been referred to as associational resistance and associational susceptibility,
45 respectively (11). Because plants are sessile, such associational resistance and
46 susceptibility are driven by plant-plant interactions among neighboring individuals
47 (11). If resistant plants repel herbivores and thereby protect susceptible neighbors,
48 associational resistance occurs rendering a mixture of resistant and susceptible plants
49 less damaged than corresponding monocultures (14, 15). In contrast, associational
50 susceptibility leads the mixture to incur more damage if herbivores are attracted to
51 susceptible plants and then spill onto resistant neighbors (8, 14). The combined
52 occurrence of associational resistance and susceptibility in a single mixture makes it
53 difficult to distinguish between positively and negatively interacting genotype pairs for
54 anti-herbivore resistance.

55 Recent studies have used standard genome-wide association studies (GWAS) to dissect
56 the genetic basis underlying beneficial plant-plant interactions (16, 17). However, it is
57 difficult to identify the most beneficial pairs among many potential pairs. In this study,
58 we aimed to predict such pairs by combining genome-wide single nucleotide
59 polymorphisms (SNPs) in *Arabidopsis thaliana* (18, 19) with a new GWAS method
60 named “Neighbor GWAS” (20). Neighbor GWAS adopts a physical model of magnets to
61 estimate locus-wise positive or negative interactions between focal and neighbor
62 individuals over randomized mixtures of many genotypes (20) (Fig. 1). We first planted
63 replicated individuals of 199 *A. thaliana* genotypes at two field sites and observed
64 naturally emerging communities of herbivores, which were analyzed as extended
65 phenotypes of the plants in standard GWAS or Neighbor GWAS. We then used Neighbor
66 GWAS as a tool to predict associational resistance or susceptibility out of all possible
67 19,701 pairs among the 199 genotypes. To test our prediction, we finally planted
68 genotypes of prospective beneficial pairs in mixtures and monocultures.

69 To enable GWAS of herbivore damage, we planted *A. thaliana* genotypes in a
70 randomized block design in two experimental gardens over two years (Table S1; Fig.
71 1A). This allowed us to monitor the abundance of 18 insect species on nearly 6400
72 individual plants (≈ 199 genotypes \times 8 blocks \times 2 sites \times 2 years) at a native (Zurich,

73 Switzerland) or exotic (Otsu, Japan) field site (Table S2; Fig. S1). We quantified
74 herbivore damage as the number of leaf holes in Zurich and leaf area loss in Otsu
75 because the major herbivores in Zurich were flea beetles and those in Otsu were
76 diamondback moths or small white butterflies (Fig. 1B; Fig. S1). To specify insect
77 functional groups responsible for herbivore damage, we quantified three extended
78 phenotypes for herbivore communities by counting individuals of external feeders (e.g.,
79 beetles in Zurich or caterpillars in Otsu), individuals of internal feeders (aphids and
80 thrips), and all insect species per plant individual (Fig. S2). All four phenotypes
81 exhibited quantitative phenotypic variation among the individual plants (Fig. S2),
82 making them suitable target phenotypes for GWAS.

83 Before using the Neighbor GWAS, we performed a standard GWAS to examine focal
84 genotype effects on herbivore damage and insect community composition. For all four
85 phenotypes, we found significant heritability among plant genotypes at both the sites
86 (likelihood ratio test, $p < 0.05$: “focal” in Fig. 1B; Fig. S3; Table S3). Regarding the effects
87 of focal genotypes on herbivore damage in Zurich (Fig. S4A; Table S4), we detected a
88 significant SNP in the *GLABRA1* gene. This gene is known to initiate leaf trichome
89 development and thereby prevent herbivory by flea beetles (21). Although previous
90 studies reported significant effects of the glucosinolate genes *GS-OH* and *MAM1* on field
91 herbivory (22), none of the measured phenotypes showed significant peaks near these
92 glucosinolate genes (Fig. S4A and S5A; Table S4). This was likely because most
93 herbivores observed in this study were specialists (Fig. S1; Table S2) and thus overcame
94 the glucosinolate defense. The results of the standard GWAS agreed with previous
95 evidence for physical defense, whereas the herbivore damage observed in our study
96 was unlikely to be attributable to the known mechanisms of defense by glucosinolates.

97 To test whether neighbor genotypes contributed to genetic variation in herbivore
98 damage, we applied the Neighbor GWAS method that considered neighbor genotype
99 effects besides the focal genotype effects (Fig. 1C) (20). The neighbor genotypes
100 explained a significant fraction of the phenotypic variation in the herbivore damage of
101 focal plants at both sites compared with focal genotype effects alone (“focal+neig.” in
102 Fig. 1B; Fig. S3; Table S3), indicating the importance of neighbor genotypes in shaping
103 herbivore damage. Additionally, we performed Neighbor GWAS of the insect community
104 composition to examine which types of insect herbivores were the most influenced by
105 neighbor genotypes. Flea beetles that could jump between plants were abundant in
106 Zurich (Fig. S1) and its abundance on focal plants was significantly influenced by
107 neighbor genotypes (Fig. 1B; Table S3). In contrast, the contribution of neighbor
108 genotypes to the number of external feeders on focal plants was not significant in Otsu
109 (Fig. 1B; Table S3), where the major external feeders were sedentary caterpillars that
110 did not move between the plants (Fig. S1). Flower thrips that can move between
111 flowering plants were abundant in Otsu (Fig. S1) and the number of internal feeders
112 including this thrip species was significantly influenced by neighbor genotypes (Fig. 1B;
113 Table S3). Reflecting the significant contributions of neighbor genotypes to either
114 external feeders in Zurich or internal feeders in Otsu, neighbor genotypes significantly

115 contributed to the total number of insect species on focal plants at both sites (Fig. 1B;
116 Fig. S3; Table S3). These patterns of herbivore damage and communities suggest that
117 neighbor genotypes are more likely to influence mobile herbivores than sedentary
118 herbivores.

119 We then asked how many loci underlay the influence of neighbor genotypes on
120 herbivore damage and herbivore communities on focal plants. To attribute the
121 phenotypic variation to each SNP, we mapped the statistical significance of the neighbor
122 genotype effect β_2 throughout the *A. thaliana* genome (Fig. 2A and B). This association
123 mapping did not detect any significant SNPs for any of the four phenotypes at each site
124 (Fig. 2A and B), though the genome-wide contribution of neighbor genotypes to
125 herbivore damage was significant (Fig. 1B). This result indicated a polygenic basis for
126 the neighbor effect on herbivore damage. Next, we examined whether associational
127 resistance was more likely than associational susceptibility. We focused on the sign of
128 the estimated neighbor genotype effects, $\hat{\beta}_2$, which represents positive or negative
129 interactions between the two alleles of paired neighbors — i.e., associational resistance
130 or susceptibility — against herbivore damage, respectively (20, 23). The top 0.1%-
131 associated SNPs of the four phenotypes per site had both negative and positive $\hat{\beta}_2$
132 without clear bias (Fig. S6A and B). This result suggests that associational resistance
133 and susceptibility are both possible, motivating us to examine the top-scoring SNPs with
134 signs of neighbor genotypic effects β_2 and other signatures.

135 To infer evolutionary patterns from the polygenic neighbor effects, we further analyzed
136 the signature of natural selection on the top 0.1% SNPs relevant to associational
137 resistance or susceptibility. Associational resistance and susceptibility represented by
138 positive and negative $\hat{\beta}_2$ corresponds to negative and positive frequency-dependent
139 selection on each SNP (23) (see also Supplementary Materials and Methods 2.1 and 2.4),
140 and thereby are hypothesized to balance and unbalance multiple alleles at a locus,
141 respectively (12, 24). We compared genome-wide signatures of balancing selection with
142 those of directional selection to test whether balancing selection is more likely
143 associated with positive $\hat{\beta}_2$. Herbivore damage at both sites and two further phenotypes
144 in Zurich had more SNPs under balancing selection and associational resistance ($\hat{\beta}_2 >$
145 0) compared with those under directional selection and associational susceptibility
146 ($\hat{\beta}_2 < 0$) (one-sided Fisher tests, $p < 0.05$: Fig. 2C and D; Fig. S6). In contrast, none of
147 the measured phenotypes showed opposite combinations i.e., a significant excess of
148 SNPs under directional selection and associational resistance over those under
149 balancing selection and associational susceptibility (one-sided Fisher test, $p > 0.05$).
150 These patterns are consistent with the hypothesis that associational resistance can
151 exert balancing selection on its responsible polymorphisms, highlighting the
152 evolutionary background of polygenic neighbor effects.

153 The polygenic neighbor effects (Fig. 2A and B) made it difficult to identify important
154 SNP predictors. We solved this problem using a genomic prediction approach (25) that
155 incorporated all SNPs together for phenotype prediction. To predict the neighbor effects

156 on herbivore damage of focal plants, we included all 1.2 million SNPs representing focal
157 genotypes and neighbor genotypes in the least absolute shrinking and selection
158 operator (LASSO) (26). With or without neighbor genotypes, LASSO prediction was
159 validated using a test dataset collected in another year. Among the four phenotypes we
160 had measured per site, the test dataset of herbivore damage in Zurich was slightly
161 better explained by the neighbor-including LASSO than by the neighbor-excluding
162 LASSO (Spearman's $\rho = 0.416$ and 0.391 , respectively: Fig. S7). This result indicates that
163 herbivore damage can be better predicted by incorporating neighbor genotypes.

164 Using neighbor genotypes as a better predictor of herbivore damage in Zurich (Fig.
165 S7A), we attempted to predict associational resistance or susceptibility to herbivore
166 damage by specialist flea beetles. We did this by extrapolating the neighbor-including
167 LASSO model to monoculture or mixture conditions *in silico*. From the neighbor-
168 including LASSO, we extracted 756 neighbor-related SNPs to extrapolate the herbivore
169 damage in Zurich (Fig. S8A and B). Assuming virtual mixture (a pair of two different
170 genotypes) or monoculture (a pair of the same genotypes) conditions, we estimated the
171 effects of two-genotype mixtures on the herbivore damage (Fig. S8C). This pairwise
172 effect size had a negative mode in its distribution (Fig. 3A), suggesting the prevalence of
173 associational susceptibility among the 199 genotypes. Furthermore, we found a
174 significant negative correlation between this pairwise effect size and estimated
175 herbivore damage under monoculture ($r = -0.37$; $p < 0.001$: Fig. S8F), indicating that
176 susceptible plant genotypes impose more damage on their counterparts when planted
177 with another genotype. Based on the pairwise effect size of the mixed planting (Fig. 3A),
178 our simulations also confirmed that herbivore damage increased with a random
179 increment in plant genotypic diversity (Fig. 3B; Fig. S8G). These results agree with those
180 of a previous meta-analysis that reported negative effects of plant genotypic diversity
181 on resistance to specialist herbivores (9). In this situation, we asked whether it would
182 nevertheless be feasible to identify genotype pairs that would result in associational
183 resistance at the stand level.

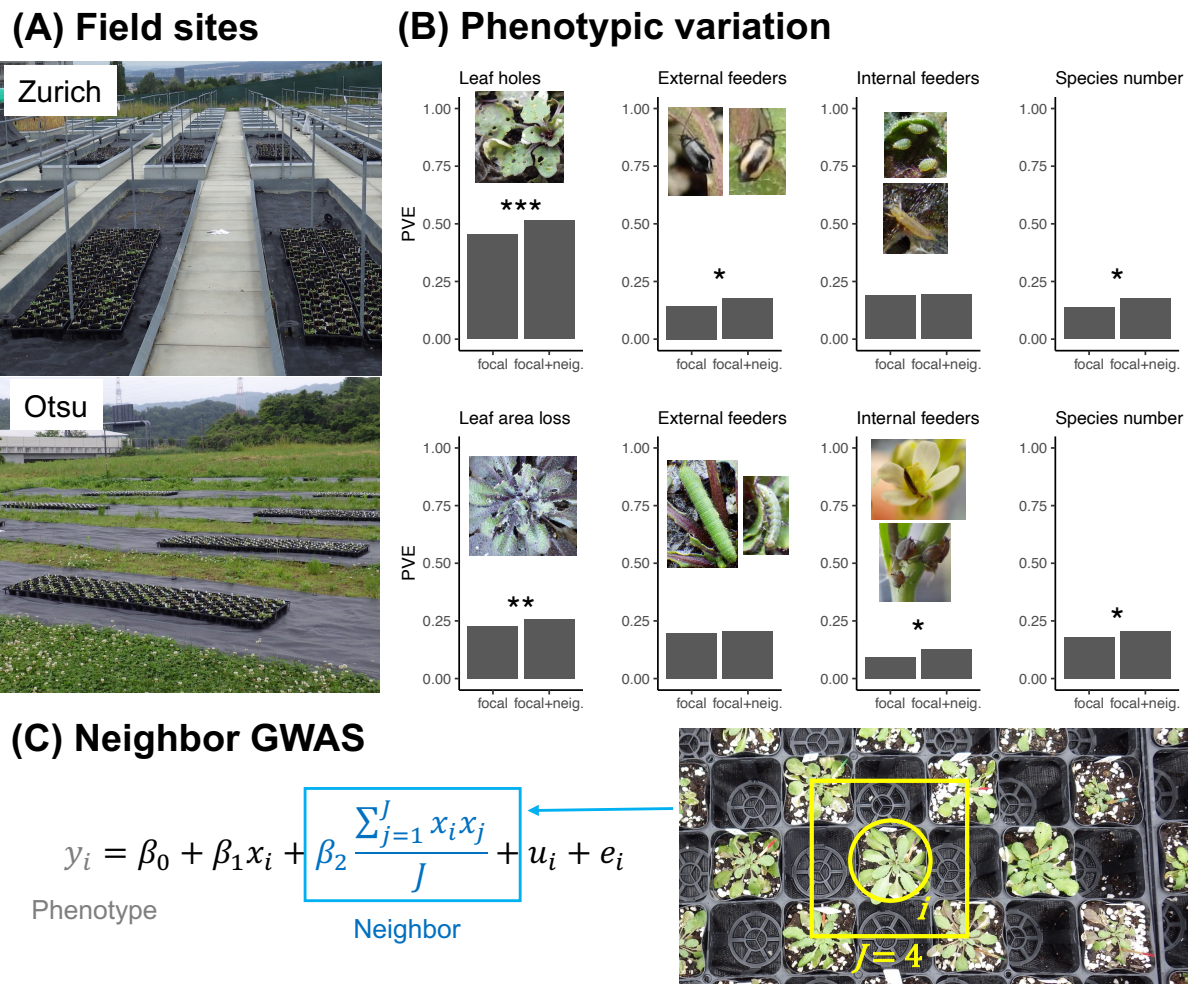
184 Despite the prevalence of negatively interacting pairs (<0 in Fig. 3A), 823 pairs had a
185 positive estimate of mixed planting (>0 in Fig. 3A). To verify associational resistance at
186 the stand level *in situ*, we planted three genotype pairs under monoculture and mixture
187 conditions at the Zurich site (Fig. S9). From the range of positive effect sizes (>0 in Fig.
188 3A), we focused on Bg-2 and Uod-1 as a pair with a large positive effect (effect size =
189 0.8); Västervik and Jm-0 as a pair with a moderate positive effect (0.23); and Bro1-6 and
190 Bla-1 as a pair with a slight positive effect (0.1). Consistent with this order of effect size,
191 Bg-2 and Uod-1 indeed showed a significant reduction in herbivore damage in the
192 mixtures in the field (Fig. 3C; Table S5; Table S6). Västervik and Jm-0 also showed a
193 significant reduction in herbivore damage in the mixture compared with the average
194 monocultures (Fig. 3C; Table S5; Table S6). Expected from their smallest effect size, Bla-
195 1 and Bro1-6 did not show a significant reduction in herbivore damage in the mixtures
196 (Fig. 3C; Table S5; Table S6). In addition to field evidence, we allowed black flea beetles
197 to feed on the three pairs in the laboratory. This additional experiment found significant

198 differences in herbivore damage between Bg-2 and Uod-1 (likelihood ratio test, $p <$
199 0.01); and between Västervik and Jm-0 ($p < 0.05$); but not between Bla-1 and Bro1-6
200 ($p = 0.35$; Fig. S10; Table S7), indicating that the least successful pair in the field could
201 not alter herbivore damage even in a small-scale experiment. Field experiments and
202 additional laboratory evidence have demonstrated that candidate genotype pairs
203 underpin associational resistance to herbivory.

204 To understand the potential mechanisms of mixed planting, we also performed gene
205 ontology enrichment analyses for the LASSO-selected SNPs relevant to associational
206 resistance ($\hat{\beta}_2 > 0$; Table S8). We detected a significant enrichment of genes related to
207 the jasmonic acid biosynthetic process (false discovery rate < 0.05 ; Table S9A),
208 including the *LIPOXIGENASE2* (*LOX2*) and *LOX6* genes (Table S8). In contrast,
209 jasmonate-related annotations did not appear when gene ontology analysis was applied
210 for LASSO-selected SNPs relevant to associational susceptibility ($\hat{\beta}_2 < 0$; Table S9B).
211 These results suggest that jasmonate-mediated defense signaling may partly explain
212 associational resistance to flea beetles. *LOX2* is particularly known as an essential gene
213 for the production of green leaf volatiles (27), which can reduce herbivory on
214 neighboring plants (15). While the complex polygenic basis of neighbor effects makes it
215 difficult to identify large-effect genes, comprehensive mutant analyses are needed to
216 isolate causative genes.

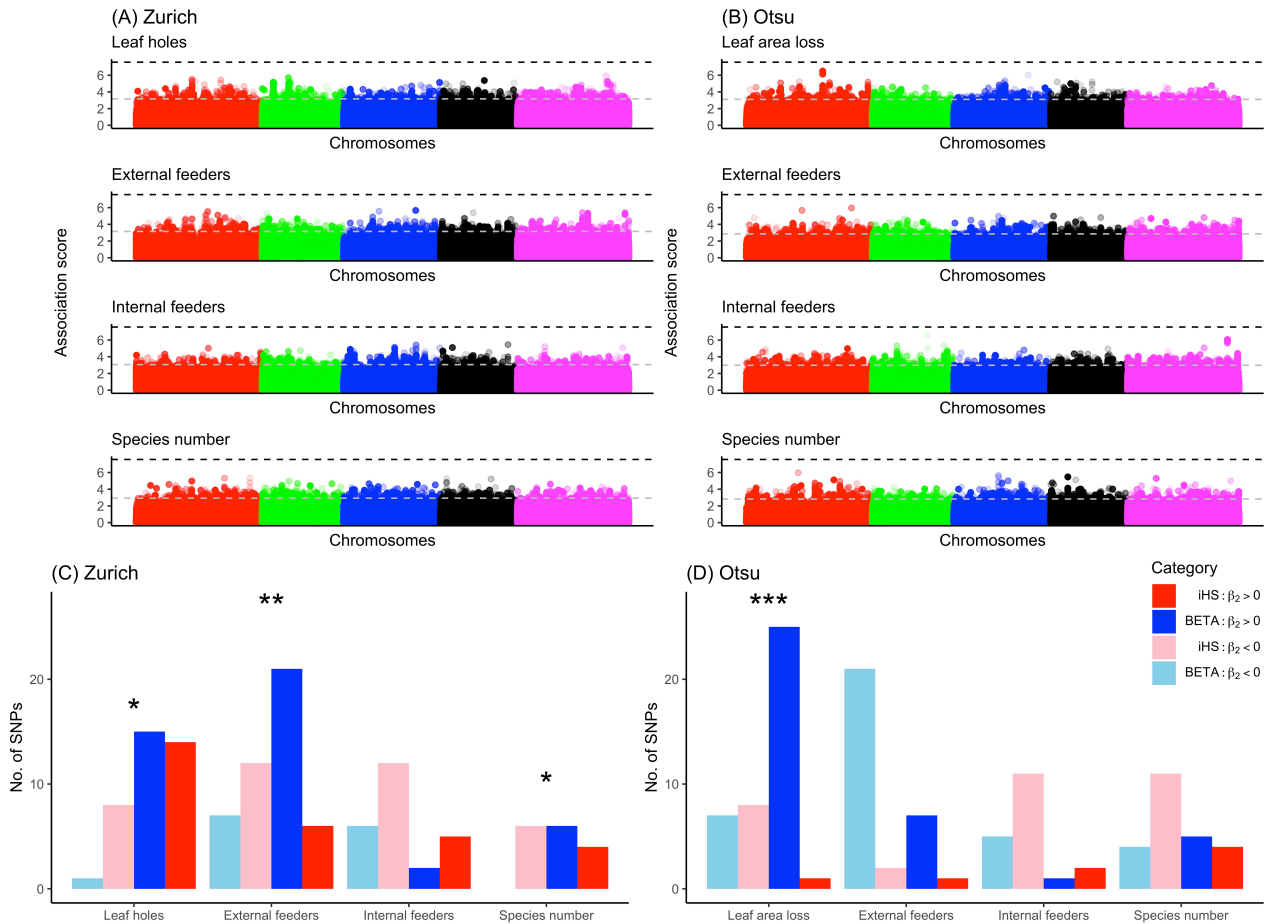
217 Our study provides a proof-of-concept to predict impacts of intraspecific mixed planting
218 on ecologically important phenotypes. Given that associational resistance has been
219 widely reported in grasslands and forests (11, 13), the present findings highlight the
220 potential ecological and evolutionary mechanisms of the effects of genetic diversity on
221 plant resistance in terrestrial ecosystems. In addition to ecological interests,
222 intraspecific mixed planting is also of applied interest because it may enhance plant
223 resistance without complicating agronomic management (17, 28, 29). The genotypes of
224 our key pair Bg-2 / Uod-1 are known to have similar flowering time (46.2 days for Bg-2
225 and 45.6 days for Uod-1 under a long-day condition) (30). This fact indicates that
226 intraspecific mixed planting can be achieved without differentiating plant life cycles that
227 may affect the timing of harvest (28). This novel strategy to identify genotype pairs with
228 beneficial mixture effects may be more widely applicable to genotype mixtures in crops
229 and other plantations.

230 **Main figures**



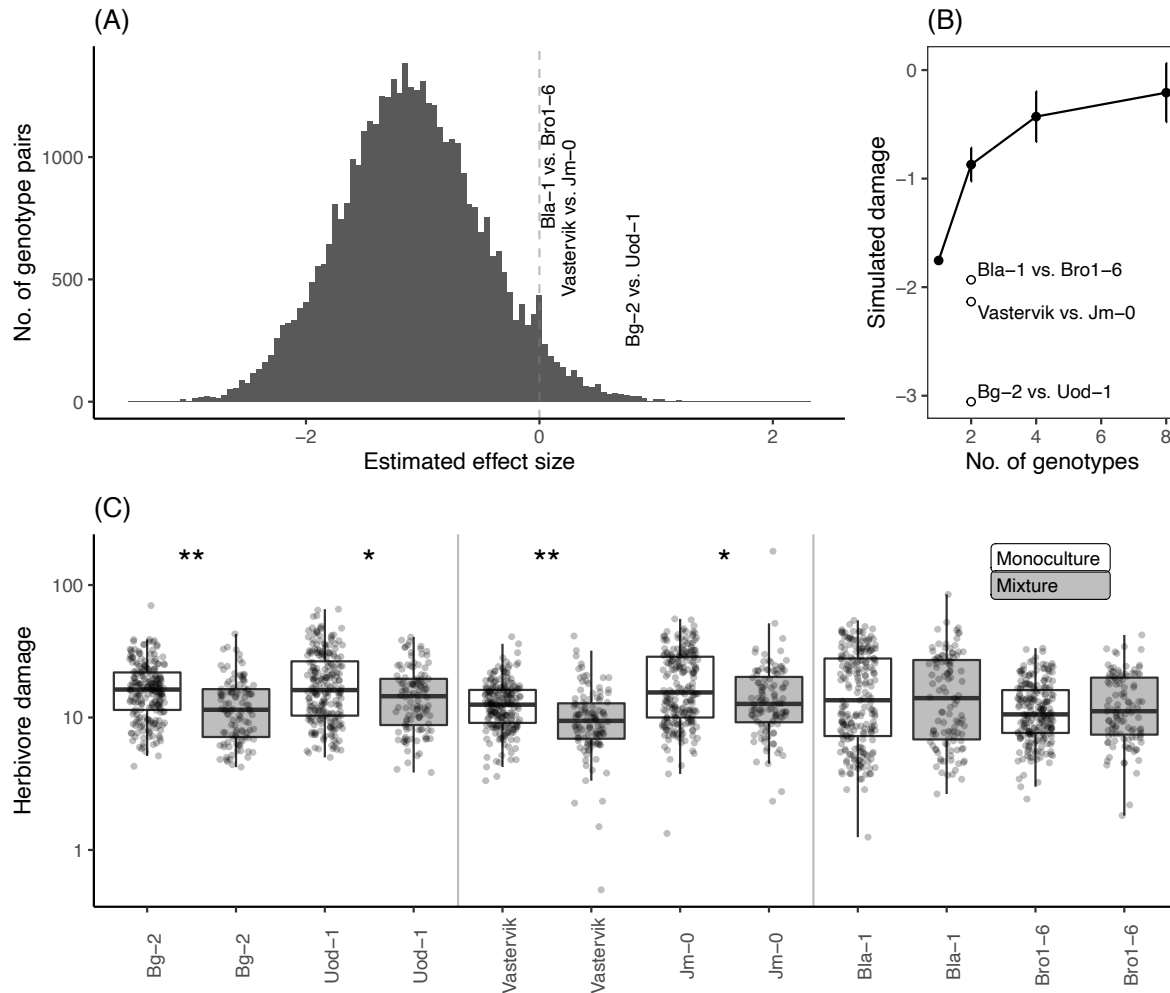
231

232 **Figure 1. Genetic variation in herbivore damage and community composition on**
 233 **randomized mixtures of *Arabidopsis thaliana* genotypes.** (A) 1,600 *A. thaliana*
 234 individuals (200 plants \times 8 randomized blocks) were planted in the Zurich or Otsu site
 235 for two years. Potted plants were arranged in a checkered manner (cf. photograph in C).
 236 (B) The proportion of phenotypic variation explained (PVE) by focal genotypes alone
 237 (focal) or both focal and neighbor genotypes (focal+neig.). Asterisks highlight the
 238 significant contributions of neighbor genotypes over those of focal genotypes: *** $p <$
 239 0.001; ** $p < 0.01$; * $p < 0.05$ (Table S3). (C) Neighbor GWAS model that includes
 240 neighbor genotype effects besides focal genotype effects. The term $(\sum_{j=1}^J x_i x_j)/J$
 241 represents the mean allele similarity between the focal (x_i) and neighbor (x_j ; j up to J)
 242 individuals. The coefficients β_1 or β_2 represent single-locus effects of the focal or
 243 neighbor genotypes on the phenotype value of the i -th focal individual y_i , respectively.



244

245 **Figure 2. Genomic basis of neighbor effects on herbivore damage and community**
 246 **composition on *Arabidopsis thaliana* genotype mixtures.** (A and B) Manhattan plots
 247 showing the $-\log_{10}(p)$ association score of the neighbor genotype effect β_2 across five
 248 chromosomes of *A. thaliana* at Zurich or Otsu. The horizontal dashed lines indicate the
 249 Bonferroni threshold at $p = 0.05$ (black) or the top 0.1% threshold of the association
 250 score (gray). (C and D) The number of SNPs shared between the selection scan (top
 251 $>5\%$) and Neighbor GWAS (top $>0.1\%$). The blue and red bars indicate balancing
 252 (BETA; blue) and directional selection (iHS; red) indices with positive (darker colors) or
 253 negative (paler colors) $\hat{\beta}_2$, respectively. Asterisks indicate a significant excess of SNPs
 254 under balancing selection between positive and negative $\hat{\beta}_2$; *** $p < 0.001$; ** $p < 0.01$;
 255 * $p < 0.05$ by Fisher tests.



256

257 **Figure 3. Effects of mixed planting on herbivore damage in silico and in situ.** (A)
258 Effect size estimates for pairwise mixed planting among the 199 *Arabidopsis thaliana*
259 genotypes. Positive and negative values indicate associational resistance and
260 susceptibility to herbivore damage, respectively. (B) Simulated damage (mean \pm SD) is
261 plotted against the number of randomly selected genotypes. (C) Herbivore damage by
262 flea beetles on the three pairs of genotypes under monoculture (white) or mixture
263 (gray) conditions in the Zurich field site. The y-axis represents the number of leaf holes
264 divided by initial plant size (no./cm). Asterisks indicate significant differences in
265 marginal means between the monoculture and mixture conditions (Table S5B): * $p <$
266 0.05 and ** $p < 0.01$.

267

268 **Supplementary Materials and Methods**

269 **Contents**

- 270 1. Field GWAS experiments
 - 271 • 1.1. Plant genotypes
 - 272 • 1.2. Field setting
 - 273 • 1.3. Phenotype survey
- 274 2. GWAS with focal and neighbor genotypic effects
 - 275 • 2.1. Neighbor GWAS model
 - 276 • 2.2. PVE and association mapping
 - 277 • 2.3. Post-GWAS analysis (i): List of candidate genes
 - 278 • 2.4. Post-GWAS analysis (ii): Selection scan
- 279 3. LASSO with focal and neighbor genotypic effects
 - 280 • 3.1. Modified Neighbor GWAS for LASSO
 - 281 • 3.2. Post-LASSO analysis (i): The effect size of mixed planting
 - 282 • 3.3. Post-LASSO analysis (ii): GO enrichment analysis
- 283 4. Mixed planting experiment
 - 284 • 4.1. Field experiment
 - 285 • 4.2. Statistical analysis
- 286 5. Laboratory choice experiment
 - 287 • 5.1. Insect materials
 - 288 • 5.2. Experimental setting
 - 289 • 5.3. Statistical analysis

290 **1. Field GWAS experiments**

291 **1.1. Plant genotypes**

292 We used *Arabidopsis thaliana* genotypes that were selfed and maintained as inbred
293 lines, called “accessions.” To study the genomic variation responsible for biotic
294 interactions, we overlapped our accessions with those used in GWAS of microbial
295 communities (31) and glucosinolates (32). We used 199 accessions with a few
296 additional accessions (Table S1), all of which were genotyped by the RegMap (18) and
297 1001 Genomes (19) projects. Seeds of these accessions were obtained from the
298 Arabidopsis Biological Resource Center (<https://abrc.osu.edu/>). The Santa-Clara
299 accession was replaced with Fja1-1 in 2018 because the genotype of Santa-Clara was
300 unavailable. For the genotype data, we downloaded a full imputed SNP matrix of 2029
301 accessions from the AraGWAS Catalog (33). Of the full 10,709,466 SNPs, we used
302 1,819,577 SNPs with minor allele frequency (MAF) at > 0.05. Our previous study
303 detected the single-gene effects of *GLABRA1* (*GL1*) on flea beetle resistance (21); thus,
304 *Ler(gl1-1)* and *Col(gl1-2)* were included to test whether our GWAS experiments worked

305 well. The *Ler* or *Col* genome was assigned to the two *gl1* mutants, with only the *GL1*
306 locus differing between the parental wild-type and *gl1* mutants.

307 **1.2. Field setting**

308 To investigate two distinct herbivore communities, we used field sites within or outside
309 a natural distribution range of *A. thaliana*. As a native site, we used the outdoor gardens
310 of the University of Zurich-Irchel campus (Zurich, Switzerland: 47° 23'N, 8° 33'E, alt. ca.
311 500 m) (Fig. 1A). As an exotic site, we used the Center for Ecological Research, Kyoto
312 University (Otsu, Japan: 35° 06'N, 134° 56'E, alt. ca. 200 m) (Fig. 1A). In the Otsu site,
313 weeds were mown before the experiment, and the surroundings were covered with
314 agricultural sheets before the experiment (Fig. 1A). In the Zurich site, each experimental
315 block was placed in a separate bed (Fig. 1A) that was not accessible to molluscan
316 herbivores.

317 Field experiments were conducted three times in 2017, 2018, and 2019. The field
318 experiment at Otsu was conducted from late May to mid-June, and that at Otsu was
319 conducted from late June to mid-July. The exact date of the field survey was annotated
320 on the original data file (34). Plants were initially grown under controlled conditions
321 and then planted in a field garden for three weeks. Seeds were sown on Jiffy-seven pots
322 (33-mm diameter), and stratified under 4 °C for a week. Seedlings were cultivated for
323 1.5 months under a short-day condition (8 h light: 16 h dark, 20 °C). Plants were then
324 separately potted in plastic pots (6 cm in diameter) filled with mixed soil of agricultural
325 composts (Profi Substrat Classic CL ED73, Einheitserde Co. in Zurich; Metro-mix 350,
326 SunGro Co., USA in Otsu) and perlites at a 3:1 L ratio. Covered with agricultural shading
327 nets, the potted plants were acclimated to field conditions for a few days. A set of the
328 199 accessions and an additional Col-0 accession — namely, 200 individuals in total —
329 was randomly assigned to each block without replacement and positioned in a
330 checkered manner (Fig. 1C). Eight blocks of the 200 accessions were set at each site on
331 2017 and 2018 for GWAS, while the three replicates were set on 2019 for the model
332 validation of LASSO (see “Modified Neighbor GWAS for LASSO” below). The blocks were
333 >2.0 m apart.

334 **1.3. Phenotype survey**

335 Insects and herbivorous collembola on individual plants were visually counted every 2–
336 3 days. These species were identified using a magnifying glass. Dwelling traces and
337 mummified aphids were also counted as proxies for the number of leaf miners and
338 parasitoid wasps, respectively. Eggs, larvae, and adults were counted for all species, as
339 long as they could be observed by the naked eye. All counts were performed by a single
340 observer (Y. Sato) during the daytime at each site. Small holes made by flea beetles were
341 counted at the Zurich site and their maximum number throughout the experiment was
342 used as an indicator of herbivore damage. This phenotyping was not applicable to Otsu,
343 because the most abundant herbivores were not flea beetles. Instead, the percentage of
344 leaf area loss was scored in Otsu at the end of the experiment as follows: 0 for no visible

345 damage, 1 for <10%, 2 for >10% and <25%, 3 for >25% and <50%, 4 for >50% and
346 <75%, and 5 for >75% of area eaten.

347 We also recorded the initial plant size and the presence/absence of inflorescences to
348 incorporate these phenotypes as covariates in the statistical analyses. Initial plant size
349 was evaluated by the length of the largest rosette leaf (mm) at the beginning of the field
350 experiment because this parameter represents the plant size at the growth stage. The
351 presence/absence of inflorescences was recorded 2 weeks after transplantation.
352 Herbivore damage was evaluated by the number of leaf holes in Zurich, and the leaf area
353 loss in Otsu as described above. The maximum number of individuals in each
354 experiment was used as an index of the abundance of each insect species.

355 In this study, we defined indices of community composition based on herbivore feeding
356 habits and species richness. Ordination analysis using the rda function of R (35) showed
357 that community composition more significantly differed between the two sites than
358 between 2017 and 2018 (redundancy analysis, $F = 401, p < 0.001$ for the sites; $F =$
359 $152, p < 0.001$ for the years: Fig. S1A); thus, we separated the dataset into Zurich and
360 Otsu. The number of external or internal feeders was defined as the total number of
361 individuals of leaf-chewing species (e.g., beetles and caterpillars) or species eating
362 internal parts of a plant (e.g., phloem-sucking aphids, cell content-sucking thrips, and
363 leaf miners). Because generalist herbivores were much fewer than specialist herbivores
364 at both the sites (Fig. S1; Table S2), specialist-generalist classification was not
365 applicable to our dataset. Carnivorous insects (e.g., parasitoid wasps and
366 aphidophagous ladybirds) were also found but were much fewer than herbivores. The
367 herbivore-carnivore ratio was thus not applicable, although these carnivorous insects
368 were taken into consideration for insect species diversity. For the index of insect
369 species diversity, we calculated the exponential Shannon diversity and Simpson
370 diversity indices in addition to the total number of species i.e., species richness.
371 However, Shannon diversity and Simpson diversity showed a discrete distribution that
372 did not suit GWAS, and only the total number of species had quantitative phenotype
373 values (Fig. S2). We therefore used the total number of species as an index of insect
374 species diversity. The analysis of insect communities was performed using the vegan
375 package (35) in R. All phenotypes except for the leaf area loss were $\ln(x+1)$ -
376 transformed to improve normality for GWAS and genomic prediction. Unless otherwise
377 stated, all figure presentations and basic statistical analyses were performed using R
378 version 3.6.1 (36).

379 **2. GWAS with focal and neighbor genotypic effects**

380 **2.1. Neighbor GWAS model**

381 To incorporate neighbor genotype identity into GWAS, we used a linear mixed model
382 that included an additional fixed and random effect, called Neighbor GWAS (20). The
383 core idea of this Neighbor GWAS method was inspired by the Ising model of
384 ferromagnetism to estimate its interaction coefficient based on the genetic similarity

385 between neighboring individuals (20). Let x_i denote the allelic status at each SNP of the
386 i -th focal plant and the j -th neighboring plants. The inbred accessions took two states as
387 $x_i \in \{-1, +1\}$. A phenotype value of the i -th focal individual plant y_i was then given as

388

$$y_i = \beta_0 + \beta_1 x_i + \beta_2 \left(\sum_{j=1}^J x_i x_j \right) / J + u_i + e_i \quad (\text{Eq. 1})$$

389 where β_0 is the intercept; $\beta_1 x_i$ is a fixed effect of the focal genotype and the same as
390 standard GWAS; and the second coefficient β_2 determines positive or negative effects
391 from the mean allelic similarity $(\sum_{j=1}^J x_i x_j) / J$ at a given locus between the focal
392 individual i and neighboring individuals j up to the total number of neighboring
393 individuals J . The random effects u_i and residuals e_i follow a normal distribution as $u_i \sim$
394 $N(\mathbf{0}, \sigma_1^2 \mathbf{K}_1 + \sigma_2^2 \mathbf{K}_2)$ and $e_i \sim N(0, \sigma_e^2)$, where σ_1^2 and σ_2^2 indicated the variance
395 component parameters for the polygenic effects from focal and neighbor genotypes,
396 respectively. \mathbf{K}_1 or \mathbf{K}_2 represents a kinship matrix among n plants given by the cross-
397 product $\mathbf{K}_1 = \mathbf{X}_1^T \mathbf{X}_1 / (q - 1)$ or $\mathbf{K}_2 = \mathbf{X}_2^T \mathbf{X}_2 / (q - 1)$, where \mathbf{X}_1 or \mathbf{X}_2 was a $q \times n$ matrix
398 that includes all focal genotype values or neighbor genotype similarity, respectively. A
399 standard GWAS model is a subset of the Neighbor GWAS model (Eq. 1). When β_2 and σ_2^2
400 was set at 0, the Neighbor GWAS model was equivalent to the standard GWAS model. In
401 the context of the magnetic model, positive or negative β_2 determines whether neighbor
402 clustering or mixture can maximize phenotype values at the population level,
403 respectively (20). In the context of the population genetic model, the positive or
404 negative β_2 respectively represent symmetric positive or negative frequency-dependent
405 selection that increases or decreases mean fitness at an intermediate frequency of the
406 two alleles, respectively (23, 37). In the case of plant defense, herbivory corresponds to
407 negative effects on plant fitness. In contrast to the interpretation of frequency-
408 dependent selection on fitness, positive β_2 represents a positive interaction that
409 decreases the negative effects on fitness, whereas negative β_2 represents a negative
410 interaction that increases the negative effects on fitness. In our study, SNPs with
411 positive β_2 had the potential to drive positive interactions that could reduce herbivore
412 damage by mixing two alleles.

413 **2.2. PVE and association mapping**

414 Using the Neighbor GWAS model (Eq. 1), we estimated the proportion of phenotypic
415 variation explained (PVE) by genetic factors and performed association mapping of the
416 SNP marker effects. The statistical significance of the variance components, σ_1^2 and σ_2^2 ,
417 or the fixed effects, β_1 and β_2 , was determined by likelihood ratio tests between models
418 with or without a single parameter. The proportion of phenotypic variation explained
419 (PVE) by the two genetic factors was defined as $\text{PVE} = (\sigma_1^2 + \sigma_2^2) / (\sigma_1^2 + \sigma_2^2 + \sigma_e^2)$. The
420 genomic heritability in the standard GWAS was given by $h^2 = \sigma_1^2 / (\sigma_1^2 + \sigma_e^2)$ when σ_2^2
421 was set to 0. Linear mixed models with variance component parameters σ_1^2 and σ_2^2 were
422 solved using the average information-restricted maximum likelihood method (38). To

423 perform association mapping, we then tested single-marker effects β_1 and β_2 using
424 eigenvalue decomposition on a weighted kinship matrix $\mathbf{K}' = \hat{\sigma}_1^2 \mathbf{K}_1 + \hat{\sigma}_2^2 \mathbf{K}_2$ (38). The
425 likelihood ratio was used to calculate p -values of each parameter based on χ^2
426 distribution with one degree of freedom. This line of GWAS analysis was implemented
427 in the rNeighborGWAS (20) package, which internally uses the gaston package (38).

428 To determine the space of neighbor effects, we conducted variation partitioning and
429 association mapping at $J = 4$ (up to the nearest neighbors) and $J = 12$ (up to the second
430 nearest neighbors). Starting from the smallest space, our previous simulations showed
431 that the optimal balance between false positive and negative detection of causative
432 SNPs was achieved when phenotypic variation explained by neighbor effects turned
433 significant (20). To anticipate this notion, we broadened the reference space of the
434 neighbor effects to the second-nearest neighbors i.e., $J = 12$. This association mapping
435 at $J = 12$ found significant SNPs regarding the leaf holes and leaf area loss (Fig. S4C and
436 Fig. S5C); however, the positions of the peaks were different from those of $J = 4$.
437 Furthermore, the neighbor effects on these phenotypes at $J = 12$ exhibited inflated p -
438 values (see quantile-quantile plots in Fig. S4C and Fig. S5C), indicating the risk of false
439 positives. The line of results at $J = 12$ indicates that the genomic basis of neighbor
440 effects cannot be further resolved by incorporating long-range neighbor effects. We
441 therefore presented the results of $J = 4$ in the main text, while including the results of
442 $J = 12$ for phenotypic variation (Fig. S3), association mapping (Fig. S4 and S5), and
443 selection scans (Fig. S6) in the Supplementary Figures and Tables.

444 **2.3. Post-GWAS analysis (i): List of candidate genes**

445 Candidate genes near SNPs with the top 0.1% p -values were searched within 10 kbp
446 around each SNP after association mapping. Functional annotation data from The
447 Arabidopsis Information Resource (TAIR) were used for the gene model and description
448 of *A. thaliana* (39).

449 **2.4. Post-GWAS analysis (ii): Selection scan**

450 To test whether associational resistance and susceptibility coincided with the
451 signatures of selection, we used two methods that detect balancing or directional
452 selection based on a sweep pattern near the target SNP (40, 41). First, the signature of
453 directional selection was analyzed using extended haplotype homozygosity (EHH) and
454 its integrated haplotype score (iHS), which were designed to detect positive selection
455 for new mutations (40). We focused on such a positive selection for directional selective
456 pressure because purifying selection i.e., negative selection results in monomorphism
457 and thus is not applicable for polymorphic sites. The EHH and iHS were calculated using
458 the rehh package (42). Second, the signature of balancing selection was analyzed using
459 the BetaScan method, which detects allele frequency correlations near the target SNP
460 (41). Default settings were applied to the rehh package and BetaScan methods. SNPs in
461 the top 5% of the empirical distributions were considered to be those under selection.
462 Ancestral alleles were determined in comparison with the whole genome sequence of *A.*

463 *lyrata*. The multiple alignment FASTA file comparing *A. thaliana* and *A. lyrata* genome
464 sequences was downloaded from the Ensembl database
465 (<ftp://ftp.ensemblgenomes.org/pub/plants>). Fisher's exact probability tests were
466 applied for a 2×2 matrix that included the number of SNPs for balancing or directional
467 selection; and for associational resistance ($\hat{\beta} > 0$) or susceptibility ($\hat{\beta} < 0$) (Fig. 2C and
468 D; Fig. S6E and F). One-sided Fisher tests were used to test the excess of balanced or
469 positively selected SNPs. We also changed the threshold of the top-scoring SNPs for
470 Neighbor GWAS at 0.5% and 1%, but these thresholds did not alter our conclusion in
471 the main text (results not shown).

472 3. LASSO with focal and neighbor genotypic effects

473 3.1. Modified Neighbor GWAS for LASSO

474 To perform multiple regressions on all SNPs, we used sparse regression that could
475 simultaneously select important SNP predictors and estimate their coefficients. The
476 Neighbor GWAS model (Eq. 1) is expressed as a multiple regression model, as follows:

477
$$\mathbf{y} = \mathbf{X}_0 \boldsymbol{\beta}_0 + \mathbf{X}_1 \boldsymbol{\beta}_1 + \mathbf{X}_2 \boldsymbol{\beta}_2 + \mathbf{e} \quad (\text{Eq. 2})$$

478 where \mathbf{y} is a phenotype vector; $\boldsymbol{\beta}_0$ is a vector including coefficients for an intercept and
479 non-genetic covariates; $\boldsymbol{\beta}_1$ and $\boldsymbol{\beta}_2$ are vectors including coefficients of focal and
480 neighbor genotype effects, respectively; \mathbf{X}_0 is a matrix that includes a unit vector and
481 non-genetic covariates for n individuals. \mathbf{X}_1 is a matrix that includes the focal genotype
482 values for n individuals and q SNP markers. \mathbf{X}_2 is a matrix that includes the neighbor
483 genotype similarity for n individuals and q SNP markers as follows:

484
$$\mathbf{X}_2 = \begin{pmatrix} \left(\sum_{j=1}^J x_{1,1} x_j \right) / J & \left(\sum_{j=1}^J x_{1,2} x_j \right) / J & \dots & \left(\sum_{j=1}^J x_{1,n} x_j \right) / J \\ \left(\sum_{j=1}^J x_{1,2} x_j \right) / J & \left(\sum_{j=1}^J x_{2,2} x_j \right) / J & \dots & \left(\sum_{j=1}^J x_{2,n} x_j \right) / J \\ \dots & \dots & \dots & \dots \\ \left(\sum_{j=1}^J x_{q,1} x_j \right) / J & \left(\sum_{j=1}^J x_{q,2} x_j \right) / J & \dots & \left(\sum_{j=1}^J x_{q,n} x_j \right) / J \end{pmatrix}$$

485 To simultaneously perform variable selection and coefficient estimation, we applied the
486 least absolute shrinkage and selection operator (LASSO) (26) to Eq. 2. Because LASSO is
487 sensitive to high correlations among explanatory variables, we further cut off 1,819,577
488 SNPs to 1,242,128 SNPs with the criterion of linkage disequilibrium (LD) at $r^2 < 0.8$
489 between adjacent SNPs. The initial plant size, presence/absence of inflorescences, and
490 experimental blocks were considered as fixed covariates. Important variables were
491 selected from 1,242,128 SNP markers and the same number of neighbor-related SNPs
492 using LASSO. We used the Python version of the glmnet package (43) to perform LASSO.

493 The kinship or population structure among individuals was implicitly considered
494 because LASSO regression could deal with all the SNPs simultaneously. While a gradient
495 of sparse regressions from the LASSO, via the elastic net, to the ridge regression was
496 available in the *glmnet* package (43), we used the sparsest regression, LASSO, because
497 of a computational burden of recursive calculation during the effect size estimation and
498 simulation (see “Effect size of mixed planting” below).

499 To determine the LASSO regularization parameter λ , we first trained the LASSO models
500 with the learning data (years 2017 and 2018) and then validated their outputs using the
501 test dataset collected in another year (i.e., 2019; see also “Field setting” above). The
502 predictability of the four phenotypes was evaluated based on the correlations between
503 the predicted and observed values of each phenotype. Spearman’s rank correlation ρ
504 was used because some phenotypic values were not normally distributed. The predicted
505 values were obtained from the LASSO models with different values of λ . To assess
506 genetically based predictability, we quantified observed phenotype values in 2019 as
507 residuals of a standard linear model. This standard linear model incorporated the same
508 non-genetic explanatory variables as the LASSO model, including the initial plant size,
509 presence of inflorescence, and difference in three experimental blocks, while each
510 phenotype was considered a response variable. To determine whether the
511 incorporation of neighbor genotypes improved the correlation with the test data, we
512 compared LASSO with or without neighbor genotypes across a series of λ . If the
513 neighbor-including LASSO yielded a larger correlation than the neighbor-excluding
514 LASSO at a given λ , this indicates that neighbor genotypes were able to improve the
515 predictability of a target phenotype by LASSO. In this context, the maximum ρ of the
516 neighbor-including LASSO was larger than that of the neighbor-excluding LASSO on
517 herbivore damage in Zurich (Fig. S7). Furthermore, the neighbor-including LASSO
518 achieved this maximum ρ even at stringent regularization (= larger λ) compared to the
519 neighbor-excluding LASSO (Fig. S7A). For the Otsu site, the neighbor-including LASSO
520 also had slightly larger correlations with herbivore damage than the neighbor-excluding
521 LASSO, supporting the improved predictability of herbivore damage by neighbor
522 genotypes at another site (Fig. S7B). None of the community composition phenotypes,
523 however, showed better predictability by the neighbor-including LASSO (Fig. S7B). This
524 was presumably because the abundance of the predominant species differed between
525 study years (Fig. S1B-G). These additional results support the improved predictability of
526 herbivore damage but suggest difficulty in predicting community composition by
527 neighbor genotypes.

528 When the neighbor-including LASSO outperformed the neighbor-excluding ones at a
529 given λ , we obtained the vectors of the estimated coefficients $\hat{\beta}_2$ that were able to
530 improve the phenotype prediction. LASSO could yield multiple sets of $\hat{\beta}_2$ across a series
531 of λ where the neighbor-including LASSO yielded larger correlations. Larger λ tend to
532 give fewer non-zero SNPs with large coefficients, while smaller λ tend to give more non-
533 zero SNPs with small coefficients. To consider the polygenic basis of neighbor effects,

534 we averaged the estimated coefficients $\hat{\beta}_2$ per SNP across the range of λ , resulting in
535 756 SNPs with non-zero β_2 for the herbivore damage in Zurich (see the main text). This
536 estimated vector of neighbor coefficients $\hat{\beta}_2$ was used to estimate the effect size.

537 **3.2. Post-LASSO analysis (i): The effect size of mixed planting**

538 To estimate the pairwise effect size of mixed planting, we extrapolated the LASSO
539 models Eq. 2 under a virtual monoculture (= a pair of the same accession) or pairwise
540 mixture (= a pair of different accessions). The pairwise effect size was determined by
541 the difference in the linear sum $[\mathbf{x}_i \otimes \mathbf{x}_j] \cdot \hat{\beta}_2 - [\mathbf{x}_i \otimes \mathbf{x}_i] \cdot \hat{\beta}_2$ between a pair of
542 accessions. The first term $[\mathbf{x}_i \otimes \mathbf{x}_j] \cdot \hat{\beta}_2$ represents the phenotype values expected from
543 different genotype vectors between the accession i and j (= pairwise mixture), whereas
544 the second term $[\mathbf{x}_i \otimes \mathbf{x}_i] \cdot \hat{\beta}_2$ represents those expected from the same genotype
545 vectors between the accession i and i (= monoculture). The element-wise product
546 $[\mathbf{x}_i \otimes \mathbf{x}_j]$ or $[\mathbf{x}_i \otimes \mathbf{x}_i]$ represents the neighbor genotype similarity between a pair of
547 different or the same accessions, respectively. Because the neighbor genotype effects
548 turned out to have a polygenic basis (Fig. 2A and B), the genotype pairs predicted by
549 many moderate-effect loci were suitable for testing the estimated effects of mixed
550 planting. In contrast, genotype pairs showing the largest effect size were selected based
551 on a few large-effect but less reliable loci. Assuming that multiple moderate-effect loci
552 could result in the effects of mixed planting, we avoided the extreme tail of the effect
553 size distribution when focusing on pairs. Also note that β_2 in the neighbor GWAS models
554 (Eqs. 1 and 2) denotes symmetric interactions between the focal i and neighbor j
555 individuals (20), and thereby $[\mathbf{x}_i \otimes \mathbf{x}_j]$ and $[\mathbf{x}_j \otimes \mathbf{x}_i]$ have the same effects on a target
556 phenotype. Even when asymmetric effects are incorporated, they do not affect the
557 *relative* differences in phenotype values between i and j (23). Thus, we focused on the
558 symmetric neighbor effects β_2 to estimate the relative effect size of a pairwise mixture
559 on a phenotype y .

560 To test whether the increasing number of plant genotypes increases or decreases
561 herbivore damage, we also simulated herbivore damage in Zurich — i.e., $\ln(\text{no. of leaf}$
562 $\text{holes}+1)$ — using the estimated vector of the neighbor coefficients $\hat{\beta}_2$. Assuming the
563 nearest neighbors in a two-dimensional lattice, we simulated mixtures of up to eight
564 genotypes. The herbivore damage was predicated by its marginal value with respect to
565 the net neighbor effects $[\mathbf{x}_i \otimes \mathbf{x}_j] \cdot \hat{\beta}_2$. To examine the overall and selected patterns, we
566 tested two types of genotype selection: (i) random selection from all pairs or (ii)
567 random selection from pairs with positive estimates of pairwise mixed planting
568 (positive values in Fig. 3A). First, eight genotypes were randomly selected out of the 199
569 accessions to represent overall pattern (Fig. 3B). We listed one (monoculture), two,
570 four, or eight (full mixture) genotype combinations among the selected eight genotypes,
571 and averaged their predicted damage $[\mathbf{x}_i \otimes \mathbf{x}_j] \cdot \hat{\beta}_2$ among all the combinations. Second,
572 four positively interacting pairs (Fig. 3A) were randomly selected to test whether
573 random selection of positive pairwise interactions could yield positive relationships

574 between genotype number and anti-herbivore resistance (Fig. S8D). Duplicates of
575 accessions were not allowed when selecting the four pairs of two paired accessions.
576 This line of random sampling was performed 9999 times to calculate the mean and
577 standard deviation. In the first case, Figure 3A shows a negative relationship between
578 the number of genotypes and plant resistance. In the second case, herbivore damage
579 decreased by paired mixing but increased by four- and eight-genotype mixing (Fig.
580 S8D). This was because scaling up pairwise mixtures to four or eight genotypes
581 confounded negatively interacting pairs. In addition to Figure 3A, these supplementary
582 results also support the difficulty in targeting positive relationships between genotype
583 richness and anti-herbivore resistance.

584 To determine whether geographical or genomic similarity could also predict the
585 pairwise effect size between *A. thaliana* accessions, we analyzed the correlations of the
586 pairwise effects with either geographical or genetic similarity. The statistical
587 significance of the Pearson correlation r between a pair of matrices was determined
588 using Mantel tests implemented in the vegan package (35) with 999 permutations. The
589 geographical distance was determined by the Euclidean distance between the latitude
590 and longitude of the locality of each accession. The locality of *A. thaliana* accessions was
591 obtained from the AraPheno database (33). The genetic distance between the two
592 accessions was determined using a kinship matrix \mathbf{K}_1 . This additional analysis
593 confirmed that the pairwise effect sizes were not related to geographical or genetic
594 distance (Mantel tests, $r = 0.02, p = 0.309$ for geographical distance; $r = -0.007, p = 1$
595 for genetic distance: Fig. S8E and F). These additional analyses indicate that the
596 estimated effect size is predictable by neither genome-wide genetic similarity nor
597 geographical origin between accessions.

598 3.3. Post-LASSO analysis (ii): GO enrichment analysis

599 To infer a category of genes related to positive and negative neighbor effects, we
600 performed gene ontology (GO) enrichment analyses for candidate genes near LASSO-
601 selected SNPs (i.e., SNPs with non-zero $\hat{\beta}_2$). Same as the post-GWAS analysis above, we
602 searched for genes within 10 kbp around each selected SNP. We then omitted
603 duplicated genes after listing the candidate genes. We finally performed Fisher's exact
604 probability tests for each GO category against the entire gene set of *A. thaliana*. Multiple
605 testing was corrected using the false discovery rate (FDR) (44). The entire set was built
606 upon the TAIR GO slim annotation (39) using the GO.db package (45) in R. To
607 summarize the results of the GO enrichment analysis, we applied the REVIGO algorithm
608 (46) to the list of significant GO terms at $FDR < 0.05$. When summarizing the significant
609 GO terms, we focused on the Biological Process with the similarity measure at 0.7 (i.e.,
610 the same as the default setting). We used the rrvgo (47) and org.At.tair.db (48) packages
611 in R to run the REVIGO algorithm. This line of GO analysis was separately performed for
612 SNPs that had negative or positive $\hat{\beta}_2$ to detect GO terms unique to positive or negative
613 neighbor effects on anti-herbivore resistance. Note also that post-GWAS GO analyses
614 possess the issue of statistical non-independence due to linkage disequilibrium in

615 standard GWAS (49). However, LASSO was unlikely to be subject to this issue because
616 (i) this sparse regression could sparsely select SNP variables across a genome; (ii) we
617 pruned adjacent SNPs on the strong LD at $r^2 > 0.8$; and (iii) we focused on unique
618 genes before using the Fisher tests. Therefore, we applied the conventional GO
619 enrichment test based on the Fisher tests with FDR correction for the LASSO results.
620 The in-house R package that includes utility functions of the GO enrichment analysis is
621 available at GitHub and Zenodo (50).

622 **4. Mixed planting experiment**

623 **4.1. Field experiment**

624 To test the effects of mixed planting on herbivore damage, we transplanted three pairs
625 of accessions (i.e., Bg-2 and Uod-1; Västervik and Jm-0; and Bla-1 and Bro1-6) under
626 mixture and monoculture conditions. The theory of plant neighbor effects suggests that
627 both plant patch size and neighbor composition should be manipulated to distinguish
628 the effects of mixed planting from the density-dependent attraction of herbivores (14).
629 We therefore set the large or small plant patches in addition to monoculture or mixture
630 conditions. The field experiment was conducted from late June to July 2019 and 2021 in
631 the outdoor garden of the University of Zurich-Irchel. Plants were first grown under
632 short-day conditions and then transferred to an outdoor garden following the same
633 procedure as the field GWAS above. Two accessions were then mixed in a checkered
634 manner under the mixture condition, while either of the two accessions was placed
635 under the monoculture conditions. The large patch included 64 potted plants in 8×8
636 trays and had a single replicate, while the small patch included 16 plants in 4×4 trays
637 and had three replicates (photo of Fig. S9). In the mixture setting, the two potted
638 accessions filled the square space in a checkered manner without a blank position
639 (photographs in Fig. S9). The total number of initial plants was two accessions \times three
640 pairs \times the mixture or monoculture \times the large or small patches \times two years = 2,016
641 individuals. Only a few pots per plot were labelled for tracking the plots in the field,
642 whereas the other pots were not labelled to blind their information. The initial plant
643 size was measured in the same manner as in the field GWAS experiment. Leaf holes
644 were counted three weeks after transplantation. Four plants died during the field
645 experiment, resulting in a final sample size of 2,012 plants.

646 **4.2. Statistical analysis**

647 We used linear mixed models to analyze the number of leaf holes because this variable
648 appeared to be normally distributed. The response variable was $\ln(x+1)$ -transformed
649 number of leaf holes per plant to improve the normality. The explanatory variables
650 were plant accession, mixture or monoculture condition, small or large patches, and
651 study years. The initial plant size, represented by the length of the largest leaf (mm),
652 was considered as an offset term. Two-way interactions were also considered among
653 the plant accessions, mixture conditions, and patch conditions. Because the large and
654 small patches had different numbers of individual plants, this imbalance was dealt with

655 using a random factor. We split the large patch by 4×4 potted plants (= the same size
656 as the small patch; see also a photo in Fig. S9), and considered these subplot differences
657 — i.e., a total of 126 subplots — as a random effect. The significance of each explanatory
658 variable was tested using Type III analysis of variance based on Satterthwaite's effective
659 degrees of freedom (51). To compare herbivore damage for each accession between the
660 mixture and monoculture conditions, we calculated marginal means for the full model
661 based on Satterthwaite's method with Sidak correction for multiple testing (52). For
662 these analyses of leaf holes, we used the lme4 (53), lmerTest (51), and emmeans (52)
663 packages in R. Box plots visualize the median with upper and lower quartile, with
664 whiskers extending to $1.5 \times$ inter-quartile range.

665 To examine the effects of patch size and year in addition to mixed planting (Fig. 3C), we
666 analyzed a separate dataset for patch conditions and study years (Fig. S9A-D; Table S6).
667 Consistent with the order of the estimated effect size (Fig. 3A), the estimated marginal
668 means across these conditions showed the largest sum of effects of mixed planting
669 between Bg-2 and Uod-1 (= 0.495 in Table S5B) and the second largest effect between
670 Västervik and Jm-0 (= 0.453 in Table S5B). The significant effects of mixed planting on
671 herbivore damage were more detectable in the large patches than in the small patches
672 (Fig. S9). The Bg-2 or Uod-1 accessions showed a significant reduction in herbivore
673 damage among five cases out of the two accessions \times two years \times two patch conditions
674 (Fig. S9; Table S6) and a marginally significant case in the small patch ($p = 0.053$ in
675 Table S6A). The Västervik or Jm-0 showed three significantly positive cases favoring the
676 reduction in herbivore damage out of the eight conditions (Fig. S9; Table S6), indicating
677 less consistency than the Bg-2 and Uod-1 pairs under diverse conditions. The Bla-1 and
678 Bro1-6 pairs did not have significantly positive cases favoring the reduction in
679 herbivore damage out of the eight conditions and even had one case of increased
680 damage by mixed planting (Fig. S9; Table S6). The main results and separate data show
681 that the magnitude of the positive mixing effect is comparable to the order of the
682 estimated effect size.

683 5. Laboratory choice experiment

684 5.1. Insect materials

685 To examine feeding by flea beetles, we conducted laboratory choice experiments using
686 one of the two major flea beetles, the black flea beetle *Phyllotreta astrachanica*. Adult *P.*
687 *astrachanica* were collected from *Brassica* spp. at the University of Zurich-Irchel. Adults
688 and larvae were reared on German turnips (Kohlrabi) following a previously
689 established protocol (54). The species of flea beetles were identified by the DNA
690 sequence of the mitochondrial gene encoding Cytochrome C Oxidase Subunit I (*COI*).
691 DNA was extracted using ZYMO RESEARCH Quick-DNA Tissue/Insect Kits (cat. no.
692 D6016). We used universal *COI* primers designed by Folmer et al. (55) for Polymerase
693 Chain Reaction (PCR) amplification under the following conditions: Initial denaturation
694 at 95 °C for 5 minutes followed by 40 cycles of 95 °C for 15 seconds, 50 °C for 30

695 seconds, 72 °C for 60 seconds and a final extension at 72 °C for 3 minutes. The PCR
696 products were sequenced by Sanger sequencing. We compared our sequences with the
697 COI sequences registered by Hendrich et al. (56), which included 15 *Phyllotreta* species
698 with several individual vouchers per species collected in Central Europe. Our sequences
699 and the registered sequences were clustered using a neighbor-joining tree and the
700 default alignment method implemented in the Qiagen CLC Main Workbench. We
701 identified species from our samples based on phylogenetic clusters. Our sequence data
702 are registered in GenBank with IDs from Q857829 to Q857834, which include three
703 individuals of black- and yellow-striped flea beetles.

704 **5.2. Experimental setting**

705 We used three pairs of six *A. thaliana* accessions, Bg-2 vs. Uod-1, Västervik vs. Jm-0, and
706 Bla-1 vs. Bro1-6. Seeds were sown on Jiffy-seven pots (33-mm diameter) and stratified
707 at 4 °C for a week. Seedlings were cultivated under long-day conditions (16 h light: 8 h
708 dark, 22/20 °C) for 3 weeks, with liquid fertilizer added a week after the start of
709 cultivation. We then allowed two adult beetles to feed on two individuals × two
710 accessions for three days under long-day conditions. The feeding arena was constructed
711 using a transparent plastic cup (129 mm in diameter and 60 mm in height) that
712 enclosed four Jiffy-potted seedlings. Excluding cups without any infestation by *P.*
713 *astrachanica*, we obtained 15-20 replicates of the feeding arena per pair.

714 **5.3. Statistical analysis**

715 We analyzed the number of leaf holes per plant as a response variable. Because the
716 number of leaf holes in this short-term laboratory experiment was zero truncated (Fig.
717 S10), we used generalized linear models with a negative binomial error and log-link
718 function. Plant accessions and arena IDs were included as the explanatory variables.
719 Likelihood ratio tests based on a χ^2 -distribution were used after checking whether the
720 ratio of residual deviance to the residual degree of freedom was nearly one. The
721 significance of each explanatory variable was tested by excluding one variable from the
722 full model. The `glm.nb` function in the MASS package in R was used for generalized
723 linear models with negative binomial errors. Likelihood ratio tests showed that flea
724 beetles showed a significant preference between Bg-2 and Uod-1; and between
725 Västervik and Jm-0; but not between Bla-1 and Bro1-6 (Table S7). The effect of the
726 experimental area on leaf holes explained deviance but was only significant in the Bg-2
727 and Uod-1 pairs (Table S7).

728 **Acknowledgements**

729 The authors thank K.K. Thomsen, L. Mohn, M. Brasser, and all members of Shimizu
730 group for help with the field setup in Zurich; G. Yumoto, L.G. Kawaguchi for field
731 assistance in Otsu; T. Tsuchimatsu for advice on GWAS during the early stage; M.
732 Yamazaki for advice on the *Arabidopsis* cultivation and molecular experiments; F. Beran

733 for advice on the barcoding of flea beetles; and J. Bascompte, M.A. Barbour, and S.E.
734 Wuest for comments on the manuscript.

735 **Author contributions**

736 Y.S.: conceptualization, project administration, investigation, data collection, formal
737 analysis, funding acquisition, draft writing, reviewing and editing; R.S.I: investigation
738 (field), reviewing and editing; K.T.: investigation (bioassay), reviewing and editing; B.S.:
739 formal analysis (mixed planting), funding acquisition, reviewing and editing; A.J.N.:
740 conceptualization, supervision, funding acquisition, reviewing and editing; K.K.S.:
741 conceptualization, supervision, funding acquisition, reviewing and editing.

742 **Funding**

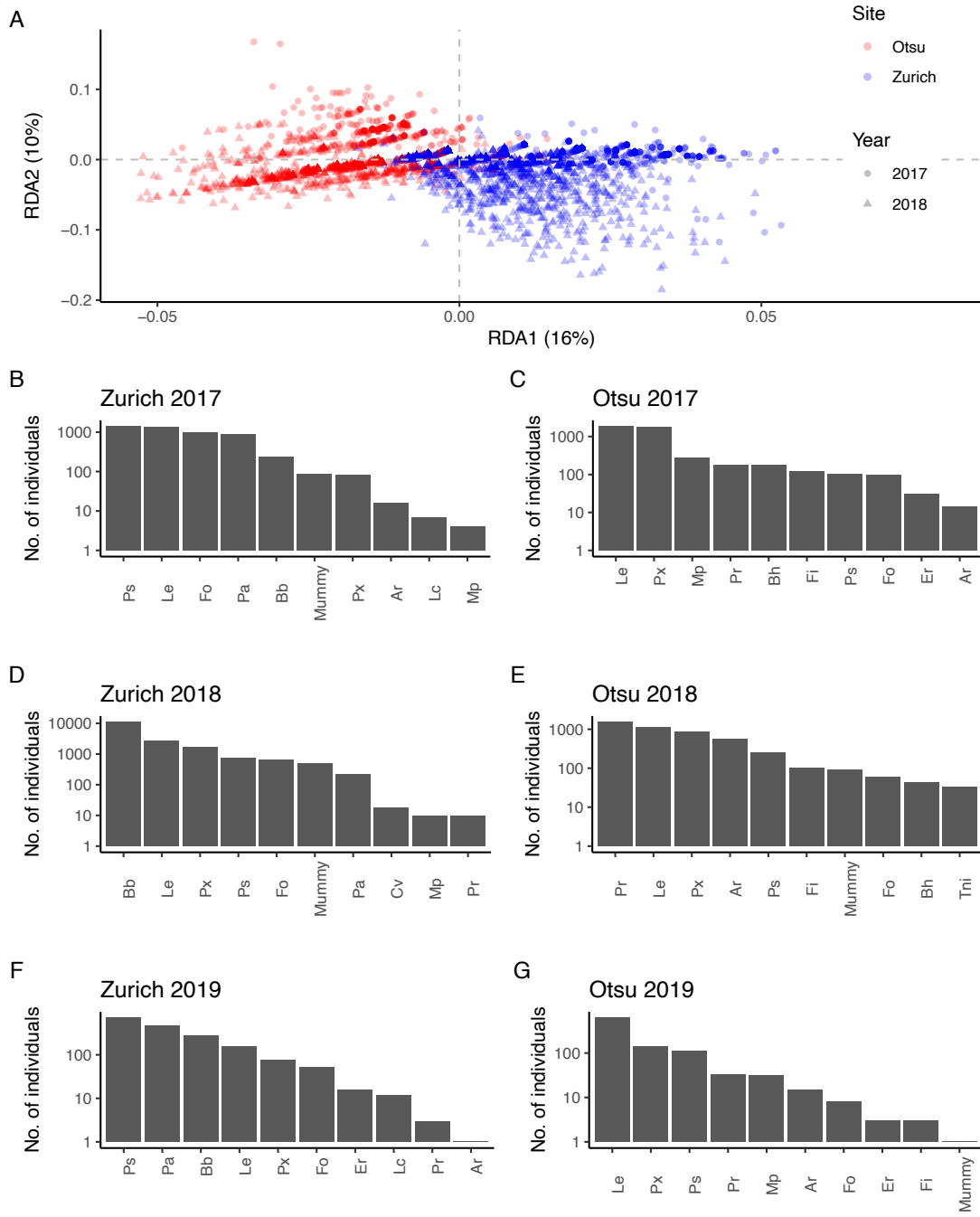
743 This study was supported by the Japan Science and Technology Agency (Grant numbers,
744 JPMJPR17Q4 to Y.S., JPMJCR16O3 to K.K.S., JPMJCR15O2 and JPMJFR210B to A.J.N.);
745 Japan Society for the Promotion of Science (JP16J30005, JP20K15880 and JP23K14270
746 to Y.S., JP20H00423 and JP23H00386 to A.J.N.); Japanese Ministry of Education, Culture,
747 Sports, Science and Technology (JP22H05179 to K.K.S., and JP23H04967 to A.J.N.);
748 Swiss National Science Foundation (31003A_182318 and 31003A_212551 to K.K.S.);
749 University Research Priority Program “Global Change and Biodiversity” from the
750 University of Zurich to B.S. and K.K.S.; and the joint usage program of the Center for
751 Ecological Research of Kyoto University.

752 **Data availability**

753 All the source codes and original data generated in this study are available in the GitHub
754 repository (<https://github.com/yassato/AraHerbNeighborGen>). This repository is also
755 deposited in Zenodo (<https://doi.org/10.5281/zenodo.7945318>) (34).

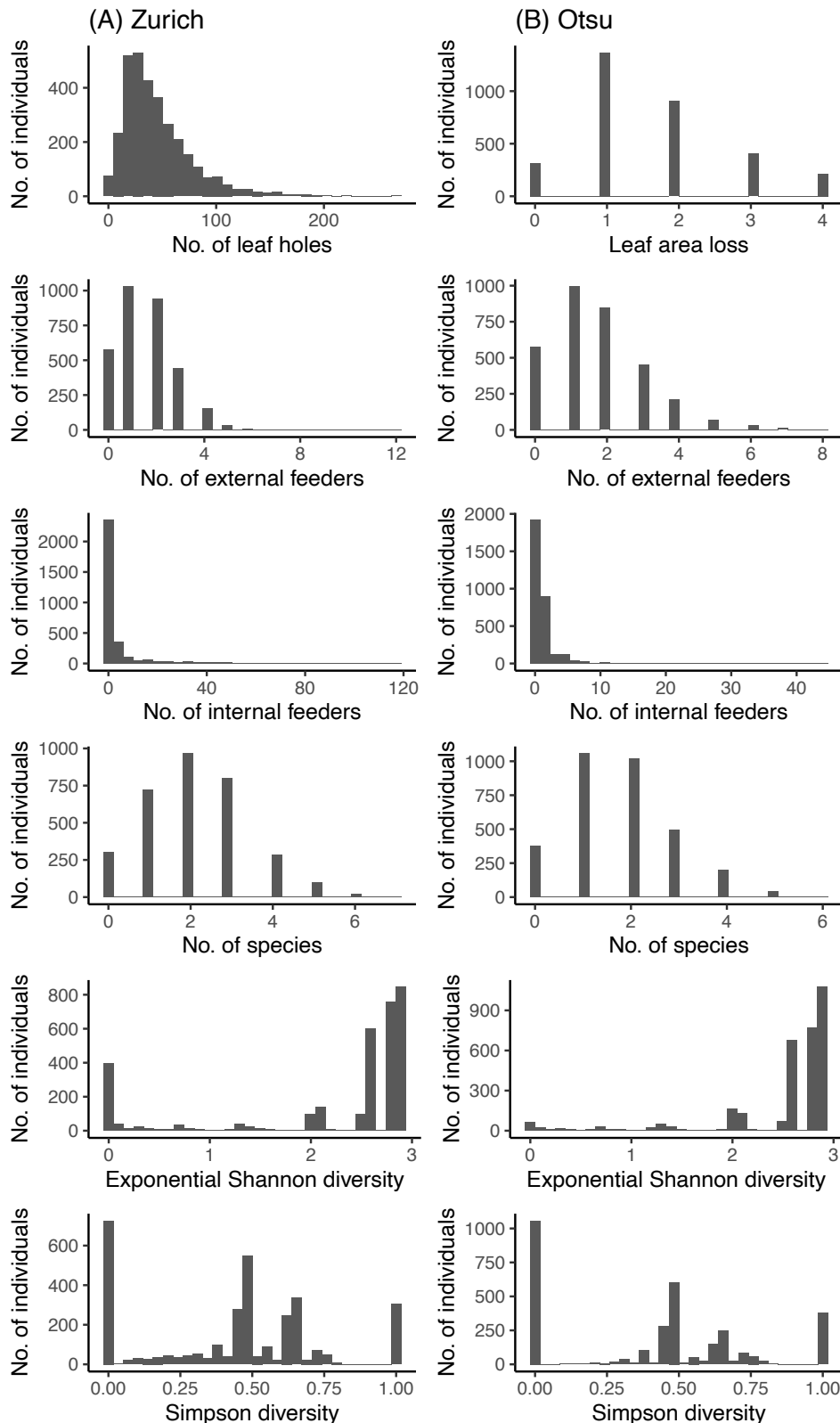
756

757 **Supplementary Figures and Tables**



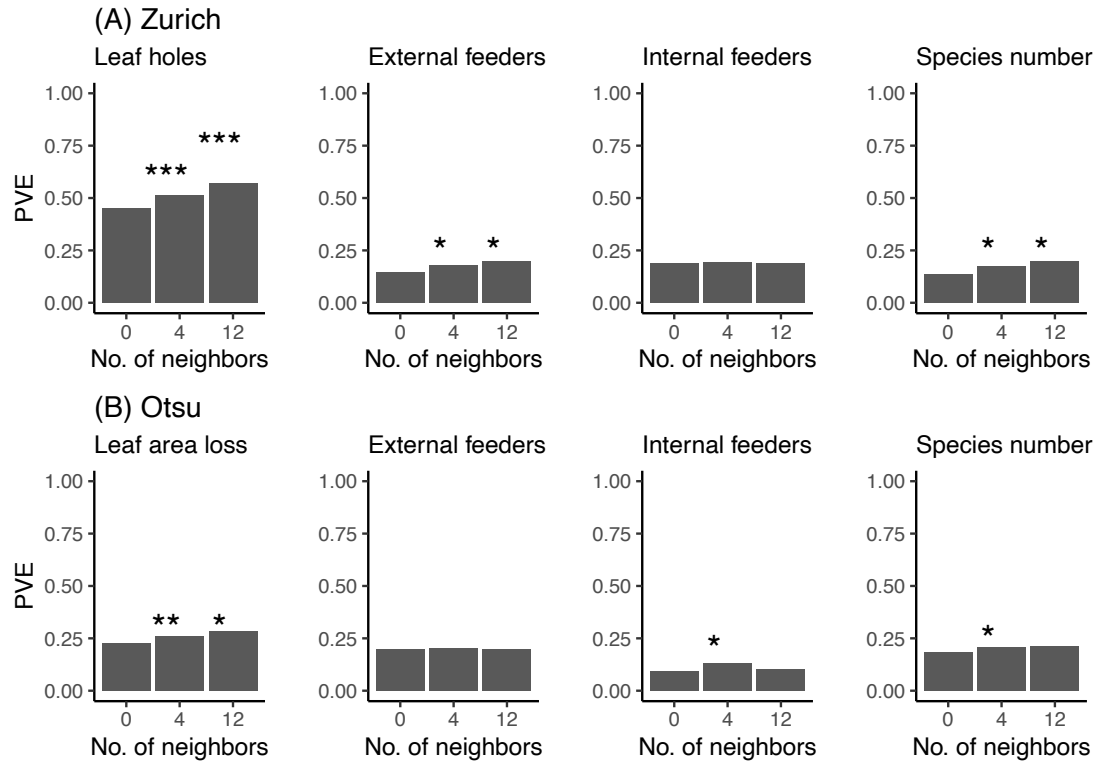
758

759 **Figure S1. Insect communities observed on field-grown *Arabidopsis thaliana* in**
 760 **Zurich and Otsu. (A)** Redundancy analysis showing the dissimilarity in insect
 761 communities between the two sites and years. The plot type indicates the study year
 762 and site: circles (2017), triangles (2018), blue (Zurich), and red (Otsu). The percentages
 763 of community variation explained by RDA1 and RDA2 are shown on each axis. (B-G)
 764 Abundance of major insect species observed from 2017 to 2019. The species name and
 765 its abbreviation correspond to those summarized in Table S2



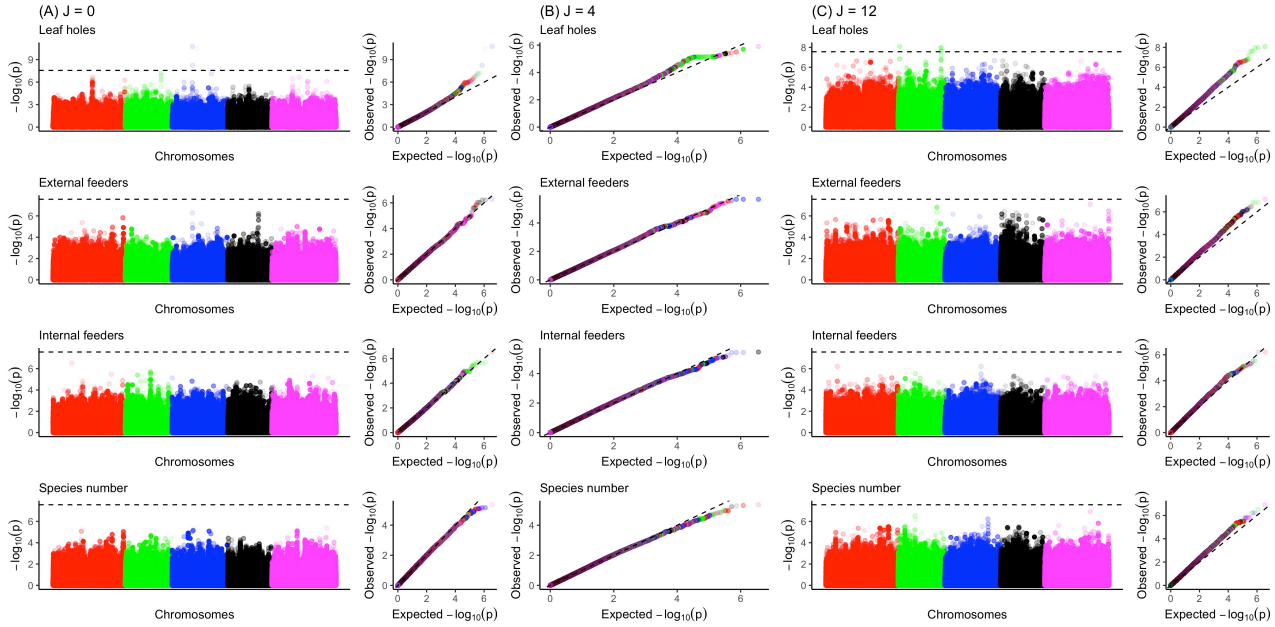
766

767 Figure S2. **Histograms of phenotypic values per plant in Zurich (A) and Otsu (B).**
768 Shown are five phenotypes subject to GWAS (the upper four rows) as well as two
769 measures of insect species diversity (the lower two rows).



770

771 **Figure S3. Proportion of phenotypic variation explained by the standard or**
772 **Neighbor GWAS model in Zurich (A) or Otsu (B).** The number of neighbors at 0
773 corresponded to the standard GWAS that quantified genomic heritability alone. The
774 numbers of neighbors J at 4 and 12 correspond to the first and second nearest
775 neighbors, respectively. Asterisks indicate the statistical significance of the neighbor
776 GWAS ($J = 4$ or 12) over standard GWAS ($J = 0$): *** $p < 0.001$; ** $p < 0.01$; * $p < 0.05$
777 with likelihood ratio tests.

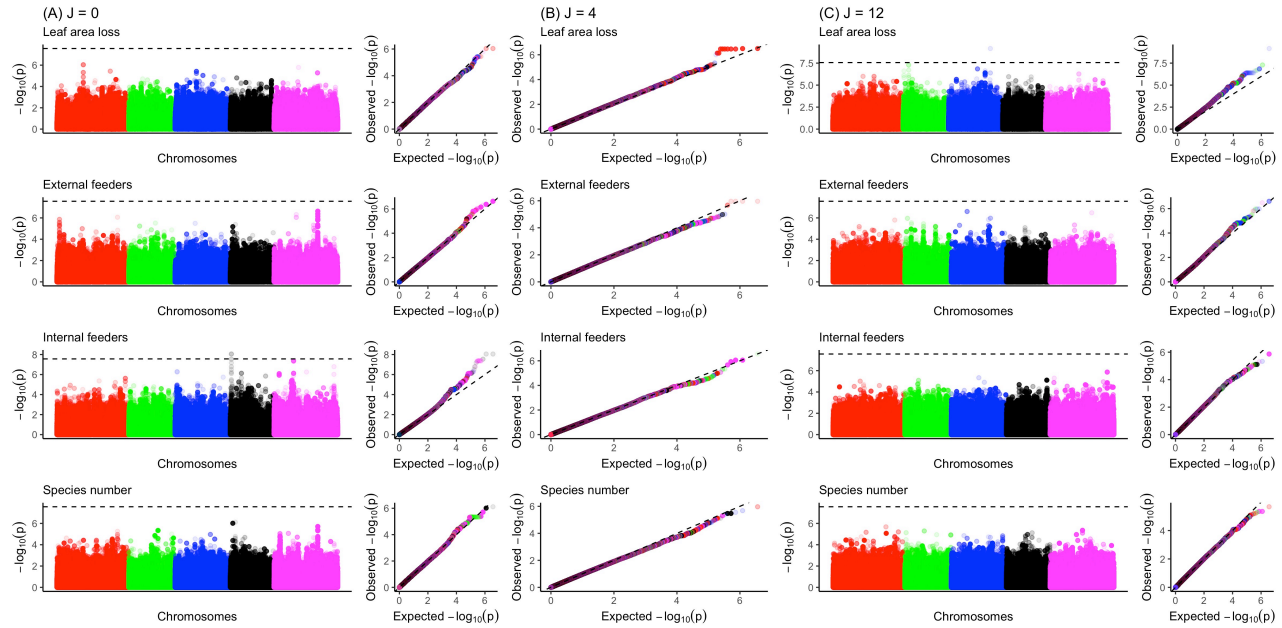


778

779 **Figure S4. Manhattan and quantile-quantile (QQ) plots for the focal genotype**
780 **effects and neighbor genotype effects on insect herbivory, abundance, and species**
781 **number in Zurich. (A) $J = 0$ (Standard GWAS); (B) $J = 4$; and (C) $J = 12$.** The
782 horizontal dashed line of the Manhattan plot indicates a genome-wide Bonferroni
783 threshold at $p = 0.05$. The gray dashed line of the QQ plots indicates the randomly
784 expected p -values. The Manhattan plots at $J = 4$ are shown in the main Figure 2A.

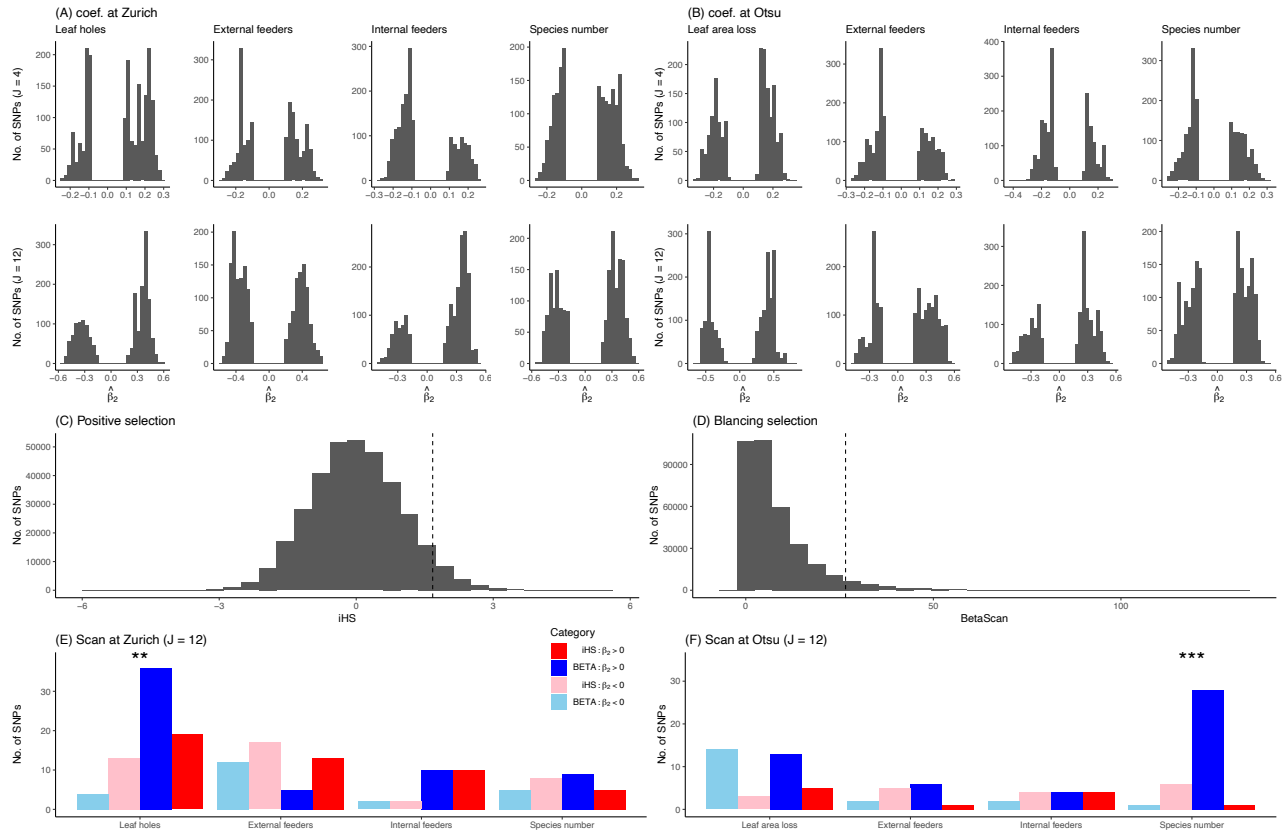
785

786



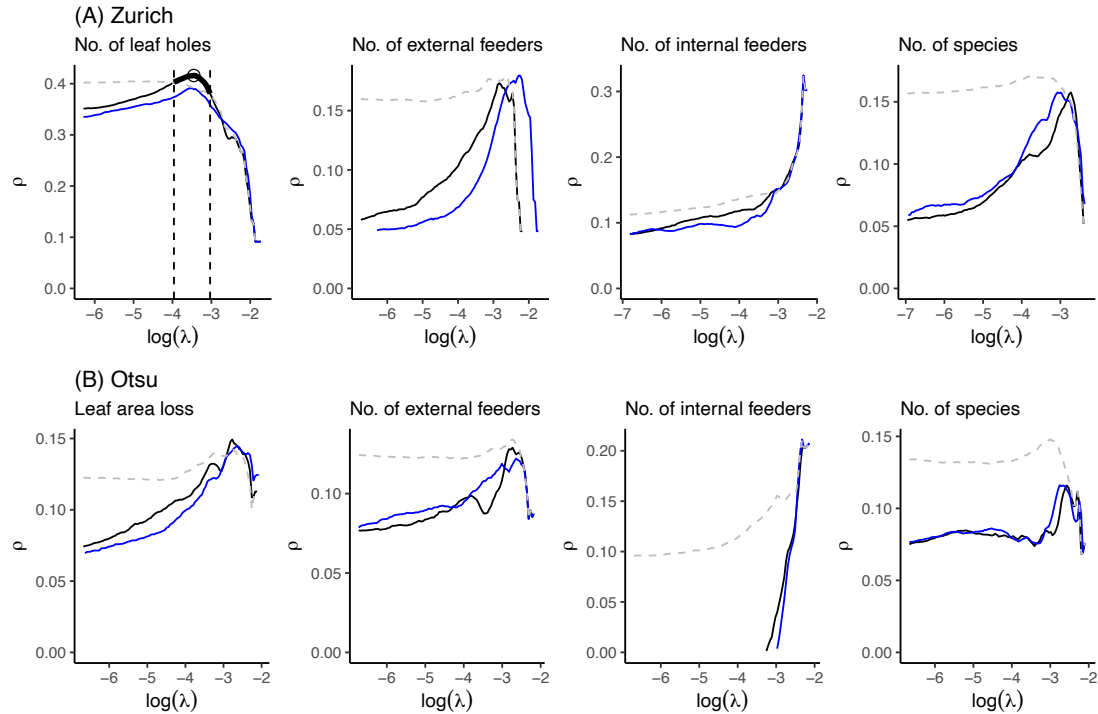
787

788 **Figure S5. Manhattan and quantile-quantile (QQ) plots for the focal genotype**
789 **effects and neighbor genotype effects on insect herbivory, abundance, and species**
790 **number in Otsu. (A) $J = 0$ (Standard GWAS); (B) $J = 4$; and (C) $J = 12$. The Manhattan**
791 **plots at $J = 4$ are shown in the main Figure 2B.**



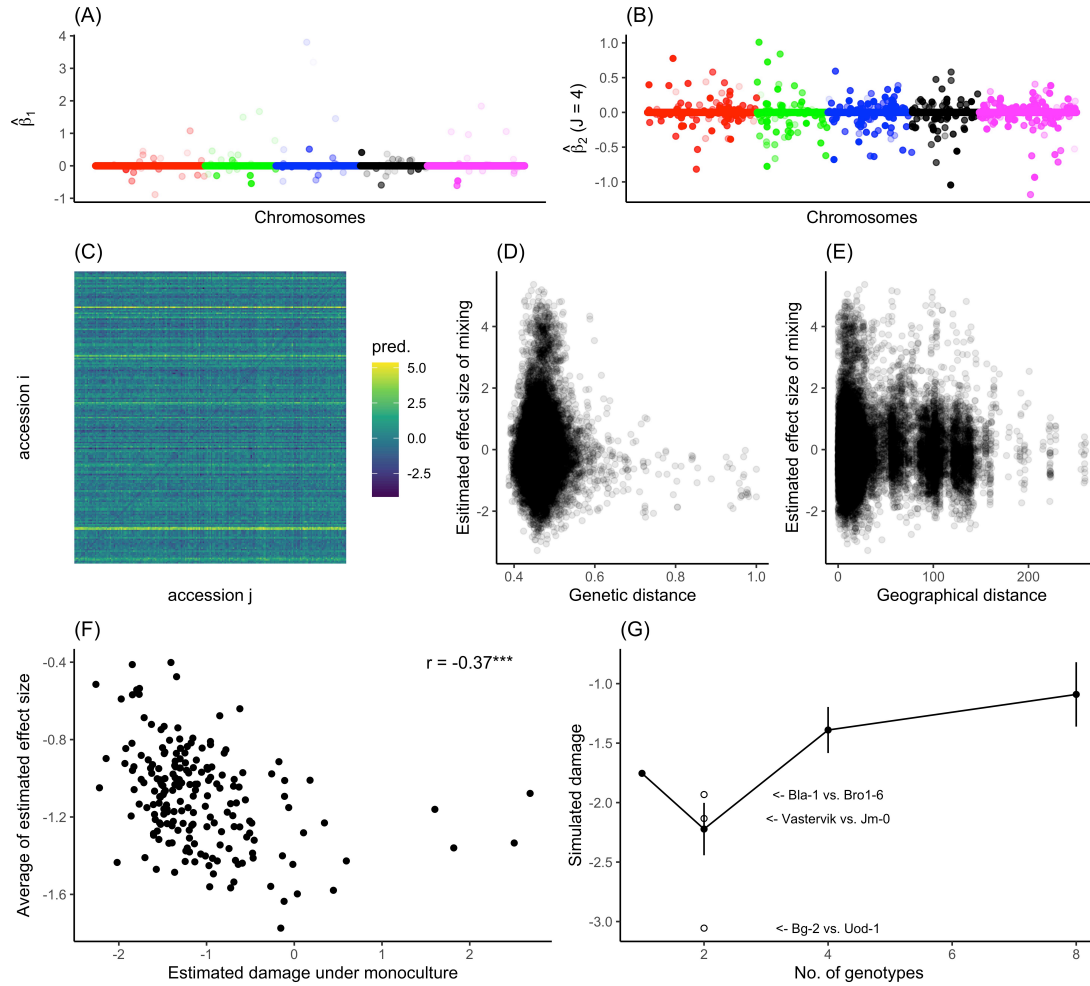
792

793 **Figure S6. Comparison of top-scoring SNPs between association mapping and**
794 **selection scans. (A and B)** Distribution of the estimated β_2 among the top 0.1%-scoring
795 GWAS SNPs. (C and D) Genome-wide distribution of the indices of positive directional
796 selection (iHS) and balancing selection (BetaScan) at MAF > 0.05. The vertical lines
797 indicate 95 percentiles. (E and F) The number of SNPs shared between the selection
798 scan (> top 5%) and the GWAS (> top 0.1%) at $J = 12$. The blue and red bars indicate
799 balancing (BETA) and positive directional selection (iHS) indices with positive (darker
800 color) or negative (paler color) $\hat{\beta}_2$, respectively. Asterisks indicate significant
801 enrichment of the balancing selection between positive and negative $\hat{\beta}_2$; *** $p < 0.001$;
802 ** $p < 0.01$ by Fisher tests.



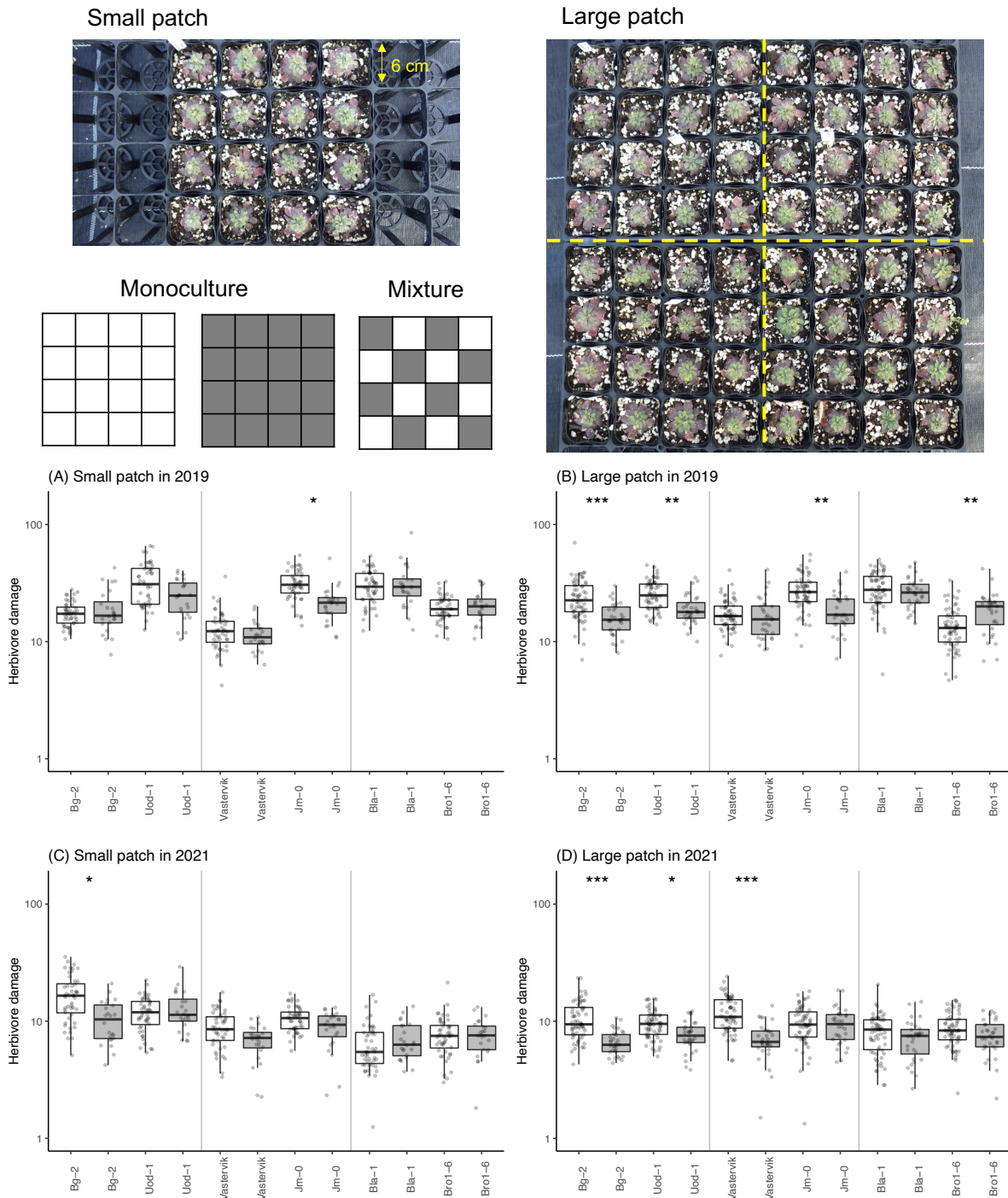
803

804 **Figure S7. Rank correlations between observed and predicted phenotypes over a**
805 **series of LASSO regularization parameters λ in (A) Zurich and (B) Otsu.** Solid lines
806 indicate the results of models including both focal and neighbor genotypes, while
807 dashed lines indicate those without neighbor genotypes. The colors of the solid lines
808 represent the reference space of the neighbor effects: $J = 4$ (black); $J = 12$ (blue). In
809 Zurich (A), neighbor-including LASSO ($J = 4$; highlighted by a bold black line) achieved
810 higher correlations with the number of leaf holes than neighbor-excluding LASSO ($J =$
811 0; gray dashed line) at more stringent regularization around the maximum ρ at $\ln(\lambda) =$
812 -3.1. An open circle highlights λ that yielded the maximum $\rho = 0.416$ for the neighbor-
813 including LASSO at $J = 4$ in addition to $\rho = 0.391$ for the neighbor-excluding LASSO at
814 $J = 0$ as mentioned in the main text. The two dashed vertical lines highlight the range of
815 λ where the neighbor-including LASSO outperformed the neighbor-excluding LASSO,
816 providing nonzero estimated SNPs in Figures S8A and B.



817

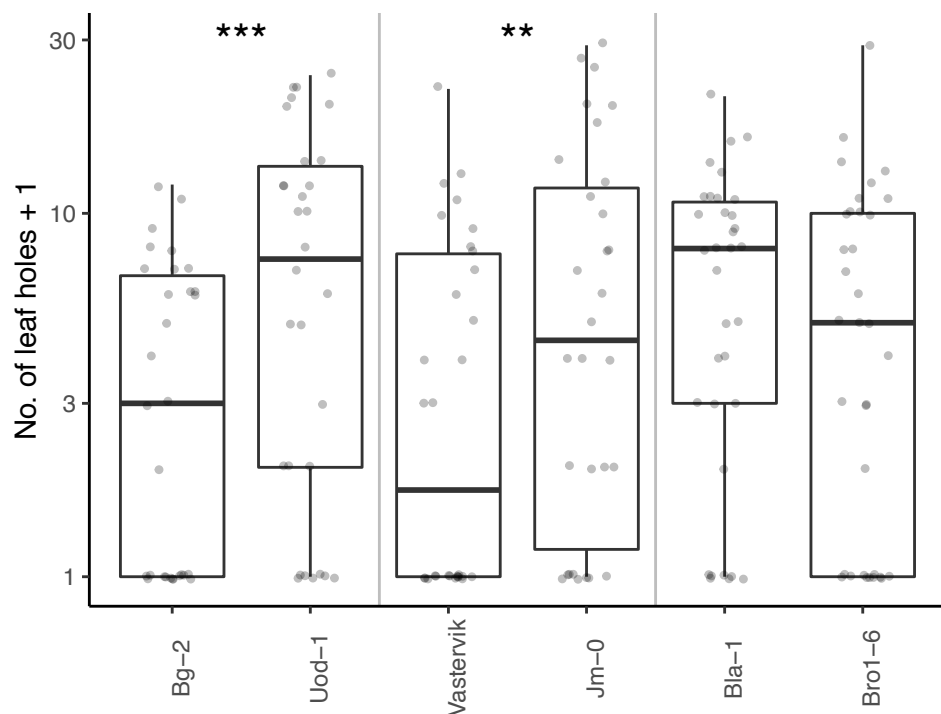
818 **Figure S8. Selected SNPs and the estimated effects of mixed planting on leaf holes**
819 **using LASSO.** Focal (A) and neighbor (B) genotype effects estimated by LASSO for leaf
820 holes at $J = 4$. (C) Heatmap showing the estimated damage between the accession i and
821 j . Diagonal elements indicate the monoculture between the same accessions i and i ,
822 while the off-diagonal elements indicate the pairwise mixture between the accession i
823 and j . (D and E) Pairwise effects plotted against the genetic distance (D) or geographical
824 distance (E) between the two accessions. (F) Estimated herbivore damage under the
825 virtual mixture condition plotted against that under monoculture conditions. A single
826 plot indicates single accession. The y-axis shows the average of the estimated effect size
827 (Fig. 3A) among 199 counterpart accessions for each focal accession on the x-axis.
828 Pearson's correction r and its level of significance from zero ($*** p < 0.001$) are also
829 shown within a plot. This negative correction became larger ($r = -0.424, *** p <$
830 0.001) when four outlier accessions were omitted from the x-axis at > 1 . (G) Predicted
831 damage (mean \pm SD) plotted against the number of randomly selected genotypes
832 showing a positive effect size in Figure 3A.



833

834 **Figure S9. Experimental settings and the effects of mixed planting on herbivore**
 835 **damage in different years and patch conditions.** The photographs display small and
 836 large patches. Yellow dashed lines in the large patches represent split subplots
 837 considered as a random effect in linear mixed models (see “Mixed planting experiment”
 838 in the Supplementary Materials and Methods). (A-D) Herbivore damage on the y-axis
 839 represents the number of leaf holes divided by the initial plant size (no./cm) on a
 840 logarithmic scale. White and gray boxes indicate the monoculture and mixture
 841 conditions, respectively. Asterisks indicate a significant difference in the estimated

842 marginal means between the monoculture and mixture conditions: ** $p < 0.01$; *** $p <$
843 0.001.



844

845 **Figure S10. Paired choice experiments using adult flea beetles and three pairs of**
846 ***Arabidopsis thaliana* accessions under laboratory conditions.** Asterisks indicate
847 significant differences between a pair of genotypes (Table S7): ** $p < 0.01$; *** $p <$
848 0.001.

849

850 Table S1. **List of *Arabidopsis thaliana* accessions used in this study** (see another file,
 851 *TableS_AccessionList.csv*).

852 Table S2. **List of arthropod species observed in this study.** NA indicates 'not
 853 applicable'. *Only this species is a non-insect arthropod. †According to *mtCOI* sequences,
 854 the yellow-striped flea beetles in Zurich included two species, *P. striolata* and *P.*
 855 *undulata*, but they could not be identified by their appearance; therefore, these two
 856 species were counted as one morpho-species in this study.

Common name	Scientific name	Order	Feeding habit	Host range	Pres./ab s. Zurich	Pres./ab s. Otsu	Abbrev.
Yellow-striped flea beetle	<i>Phyllotreta striolata</i> †	Coleoptera	Chewer	Oligophagous	+	+	Ps
Black flea beetle	<i>Phyllotreta astrachanica</i>	Coleoptera	Chewer	Oligophagous	+	-	Pa
Cabbage flea beetle	<i>Psylliodes punctifrons</i>	Coleoptera	Chewer	Oligophagous	-	+	Pp
Vegetable weevil	<i>Listroderes costirostris</i>	Coleoptera	Chewer	Polyphagous	-	+	Lc
Diamondback moth	<i>Plutella xylostella</i>	Lepidoptera	Chewer	Oligophagous	+	+	Px
Small cabbage white butterfly	<i>Pieris rapae</i>	Lepidoptera	Chewer	Oligophagous	+	+	Pr
Cabbage looper	<i>Trichoplusia ni</i>	Lepidoptera	Chewer	Polyphagous	+	+	Tn
Turnip sawfly	<i>Athalia rosae</i>	Hymenoptera	Chewer	Oligophagous	+	+	Ar
Garden springtail*	<i>Bourletiella hortensis</i>	Collembola	Chewer	Polyphagous	+	+	Bh
Cabbage bug	<i>Eurydema rugosa</i>	Hemiptera	Sucker	Oligophagous	-	+	Er
Green peach aphid	<i>Myzus persicae</i>	Hemiptera	Sucker	Polyphagous	+	+	Mp
Mustard aphids	<i>Lipaphis erysimi</i>	Hemiptera	Sucker	Oligophagous	+	+	Le
Cabbage aphids	<i>Brevicoryne brassicae</i>	Hemiptera	Sucker	Oligophagous	+	-	Bb
Flower thrip	<i>Frankliniella intonsa</i>	Thysanoptera	Sucker	Polyphagous	+	+	Fi
Western flower thrip	<i>Frankliniella occidentalis</i>	Thysanoptera	Sucker	Polyphagous	+	+	Fo
Diamondback moth	<i>Cotesia vestalis</i>	Hymenoptera	Carnivore	NA	+	+	Cv

Common name	Scientific name	Order	Feeding habit	Host range	Pres./ab s. Zurich	Pres./ab s. Otsu	Abbrev.
parasitoid							
Larvae of hoverfly	Syrphinae sp.	Diptera	Carnivore	NA	+	+	Sy
Seven-spot ladybird	<i>Coccinella septempunctata</i>	Coleoptera	Carnivore	NA	+	+	Cs
(Parasitoid wasp indicated by mummified aphids)	NA	Hymenoptera	Carnivore	NA	+	+	mummy

858 Table S3. **Likelihood ratio tests for variance component parameters in the**
 859 **standard and Neighbor GWAS.** The deviance at $J = 0$ was tested against the null
 860 deviance, and the deviance at $J = 4$ and 12 was tested that at $J = 0$. Abbreviations: PVE,
 861 proportion of phenotypic variation explained by genetic factors; DF, degree of freedom;
 862 LL, log-likelihood. Bold values highlight $p < 0.05$.

Site	Phenotype	J	$\hat{\sigma}_1^2$	$\hat{\sigma}_2^2$	$\hat{\sigma}_e^2$	PVE	DF	LL	Deviance	χ^2	p
Zurich	Leaf holes	null	0	0	1	0	3144	-963.1	1926.2	NA	NA
		0	0.4	0	0.5	0.45	314	-805.3	1610.6	315.	1.26E-7
		5		4	3	3					70
		4	0.3	0.17	0.5	0.51	314	-794.4	1588.8	21.8	3.09E-06
		7		1	3	2					
		12	0.2	0.43	0.5	0.57	314	-785.6	1571.3	39.3	3.66E-10
		6		1	3	2					
		0	0.1	0	0.8	0.14	314	-1404.4	2808.9	38.4	5.77E-10
		4		4	4	3					
		4	0.0	0.10	0.8	0.17	314	-1401.4	2802.9	6.0	1.44E-02
		8		3	7	2					
		12	0.0	0.16	0.8	0.20	314	-1401.4	2802.9	6.0	1.44E-02
		5		3	0	2					
	External feeder	null	0	0	1	0	3144	-1423.6	2847.3	NA	NA
		0	0.1	0	0.8	0.14	314	-1404.4	2808.9	38.4	5.77E-10
		4		4	4	3					
		4	0.0	0.10	0.8	0.17	314	-1401.4	2802.9	6.0	1.44E-02
		8		3	7	2					
		12	0.0	0.16	0.8	0.20	314	-1401.4	2802.9	6.0	1.44E-02
		5		3	0	2					
	Internal feeder	null	0	0	1	0	3144	-1264.4	2528.9	NA	NA
		0	0.1	0	0.7	0.19	314	-1238.2	2476.5	52.4	4.52E-13
		8		5	1	3					
		4	0.17	0.01	0.75	0.194	3142	-1238.2	2476.4	0.1	0.8103
		12	0.18	0.00	0.75	0.191	3142	-1238.2	2476.5	0.0	1
	Species number	null	0	0	1	0	3144	-1286.6	2573.2	NA	NA
		0	0.1	0	0.7	0.13	314	-1272.0	2544.90	29.2	6.37E-08
		2		7	6	3					
		4	0.0	0.09	0.7	0.17	314	-1269.6	2539.2	4.8	0.0284
		7		6	5	2					
		12	0.0	0.15	0.7	0.19	314	-1269.3	2538.7	5.3	0.0211
		4		6	7	2					
Otsu	Leaf area loss	null	0	0	1	0	3167	-1466.7	2933.4	NA	NA
		0	0.2	0	0.8	0.22	316	-1427.8	2855.7	77.7	1.20E-18
		4		4	6	6					
		4	0.1	0.12	0.8	0.25	316	-1424.1	2848.3	7.4	0.0066
		7		2	9	5					
		12	0.1	0.18	0.8	0.28	316	-1425.0	2850.0	5.6	0.0176
	External	null	0	0	1	0	3167	-1365.6	2731.2	NA	NA

Site	Phenotype	J	$\hat{\sigma}_1^2$	$\hat{\sigma}_2^2$	$\hat{\sigma}_e^2$	PVE	DF	LL	Deviance	χ^2	p
	feeder										
		0	0.2	0	0.7	0.19	316	-1329.0	2657.9	73.3	1.11E-17
			0		9	9	6				
		4	0.18	0.02	0.79	0.204	3165	-1328.8	2657.6	0.4	0.5467
		12	0.20	1.00E-06	0.79	0.199	3165	-1329.0	2657.9	0.0	1
	Internal feeder	null	0	0	1	0	3167	-1562.8	3125.6	NA	NA
		0	0.1	0	0.9	0.09	316	-1553.1	3106.2	19.4	1.09E-05
			0		3	4	6				
		4	0.0	0.10	0.9	0.12	316	-1550.3	3100.6	5.6	0.017
			2		1	9	5				
		12	0.08	0.03	0.93	0.103	3165	-1553.1	3106.1	0.1	0.7086
	Species number	null	0	0	1	0	3167	-	2735.6	NA	NA
		0	0.1	0	0.8	0.18	316	-	2670.0	65.6	5.58E-16
			8		0	1	6	1335.0			
		4	0.1	0.10	0.7	0.20	316	-1331.9	2663.7	6.3	0.012
			0		8	6	5				
		12	0.10	0.11	0.79	0.212	3165	-1333.5	2667.1	3.0	0.0844

864 Table S4. **List of candidate genes from GWAS of insect herbivory, abundance, and**
 865 **species number in the Zurich and Otsu site.** The possibility of positive or balancing
 866 selection was also annotated to each SNP (see another file, *TableS_GWAScandidate.xlsx*).

867 Table S5. **Linear mixed models for analyzing the effects of mixed planting on leaf**
 868 **holes.** (A) Analysis of variance (ANOVA) comparing models with or without a single
 869 explanatory variable. (B) Estimated marginal means of the effects of the mixture
 870 conditions in the full model. The positive estimates indicated an increase in the number
 871 of leaf holes in the monoculture relative to the mixture conditions. Bold values highlight
 872 $p < 0.05$. Abbreviations: DF: degree of freedom; SE: standard error.

873 (A) Type III nested ANOVA

<i>Explanatory variable</i>	<i>Sum of squared</i>	<i>Mean squared</i>	<i>Numerator DF</i>	<i>Denominator DF</i>	<i>F</i>	<i>p</i>
Study year	44.022	44.022	1	111.05	396.190	2.20E-16
Patch size	0.172	0.172	1	111.06	1.551	0.215626
Mixture condition	1.208	1.208	1	111.06	10.876	0.001309
Genotype	7.765	1.553	5	142.78	13.977	4.06E-11
Patch \times Mix	0.062	0.062	1	111.06	0.561	0.455632
Patch \times Geno	1.675	0.335	5	276.2	3.015	0.011464
Mix \times Geno	1.053	0.211	5	141.38	1.895	0.098884

874 (B) Estimated marginal means

<i>Genotypes</i>	<i>Estimate</i>	<i>SE</i>	<i>DF</i>	<i>t-value</i>	<i>adjusted p</i>
Bg-2	0.307	0.093	125	3.30	0.0013
Uod-1	0.188	0.093	125	2.02	0.0455
Vastervik	0.246	0.093	125	2.64	0.0093
Jm-0	0.207	0.093	125	2.22	0.0282
Bla-1	-0.058	0.093	125	-0.62	0.536
Bro1-6	0.011	0.093	125	0.12	0.905

875

876 Table S6. **Linear mixed models for analyzing the effects of mixed planting on leaf**
 877 **holes under different patch conditions over two years.** As shown in Table S5, the
 878 upper and lower tables of each panel display the results of the analysis of variance and
 879 estimated marginal means, respectively. Bold values highlight $p < 0.05$.

880 (A) Small patch in 2019

Explanatory variable	Sum of squared	Mean squared	Numerator DF	Denominator DF	F	p
Mixture condition	0.2535	0.25348	1	18.025	2.6619	0.1201
Genotype	15.4601	3.09201	5	26.911	32.4703	1.37E-10
Mix × Geno	0.9509	0.19017	5	26.911	1.9971	0.1113

881

Genotypes	Estimate	SE	DF	t-value	adjusted p
Bg-2	-0.038	0.136	22.6	-0.28	0.783
Uod-1	0.277	0.136	22.6	2.04	0.053
Vastervik	0.093	0.136	22.6	0.69	0.500
Jm-0	0.366	0.136	22.6	2.70	0.013
Bla-1	-0.028	0.136	22.6	-0.21	0.838
Bro1-6	-0.042	0.136	23.1	-0.31	0.761

882 (B) Large patch in 2019

Explanatory variable	Sum of squared	Mean squared	Numerator DF	Denominator DF	F	p
Mixture condition	1.0855	1.08555	1	27.114	8.8754	0.006031
Genotype	14.049	2.80979	5	51.573	22.9728	4.71E-12
Mix × Geno	3.9201	0.78403	5	51.573	6.4102	0.000106

883

Genotypes	Estimate	SE	DF	t-value	adjusted p
Bg-2	0.3653	0.0951	43.2	3.84	0.0004
Uod-1	0.2873	0.0951	43.2	3.02	0.0042
Vastervik	0.0544	0.0951	43.2	0.572	0.5701
Jm-0	0.2952	0.0951	43.2	3.103	0.0034
Bla-1	0.0508	0.096	44.6	0.53	0.5988
Bro1-6	-0.2971	0.0951	43.2	-3.123	0.0032

884 (C) Small patch in 2021

<i>Explanatory variable</i>	<i>Sum of squared</i>	<i>Mean squared</i>	<i>Numerator DF</i>	<i>Denominator DF</i>	<i>F</i>	<i>p</i>
Mixture condition	0.16583	0.16583	1	18	1.6168	0.219727
Genotype	2.70265	0.54053	5	22.208	5.2699	0.002441
Mix × Geno	0.76187	0.15237	5	22.208	1.4856	0.234422

885

<i>Genotypes</i>	<i>Estimate</i>	<i>SE</i>	<i>DF</i>	<i>t-value</i>	<i>adjusted p</i>
Bg-2	0.4537	0.207	19.9	2.188	0.0408
Uod-1	-0.0631	0.207	19.9	-0.304	0.7642
Vastervik	0.273	0.207	19.9	1.316	0.203
Jm-0	0.2121	0.207	19.9	1.023	0.3188
Bla-1	-0.1145	0.207	19.9	-0.552	0.5869
Bro1-6	0.0101	0.207	19.9	0.049	0.9618

886 (D) Large patch in 2021

<i>Explanatory variable</i>	<i>Sum of squared</i>	<i>Mean squared</i>	<i>Numerator DF</i>	<i>Denominator DF</i>	<i>F</i>	<i>p</i>
Mixture condition	2.6127	2.61273	1	27	23.2567	4.91E-05
Genotype	1.0728	0.21455	5	44.912	1.9098	0.111524
Mix × Geno	2.4543	0.49086	5	44.912	4.3693	0.002517

887

<i>Genotypes</i>	<i>Estimate</i>	<i>SE</i>	<i>DF</i>	<i>t-value</i>	<i>adjusted p</i>
Bg-2	0.4157	0.109	37.2	3.82	0.0005
Uod-1	0.2275	0.109	37.2	2.091	0.0435
Vastervik	0.5491	0.109	37.2	5.046	<.0001
Jm-0	0.0121	0.109	37.2	0.111	0.9121
Bla-1	0.1089	0.109	37.2	1	0.3236
Bro1-6	0.1398	0.109	37.2	1.284	0.207

888

889 Table S7. **Generalized linear models analyzing the number of leaf holes in paired**
890 **choice experiments.** Likelihood ratio tests based on the deviance and χ^2 -distribution
891 are shown for the three pairs of genotypes. Bold values highlight $p < 0.05$.

892 (A) Bg-2 vs. Uod-1

<i>Explanatory variable</i>	<i>DF</i>	<i>Deviance</i>	<i>p</i>
Arena	14	25.42	0.031
Genotype	1	13.35	0.0003
Residual	44	69.36	—

893 (B) Vastervik vs. Jm-0

<i>Explanatory variable</i>	<i>DF</i>	<i>Deviance</i>	<i>p</i>
Arena	14	20.89	0.105
Genotype	1	5.71	0.017
Residual	44	64.57	—

894 (C) Bla-1 vs. Bro1-6

<i>Explanatory variable</i>	<i>DF</i>	<i>Deviance</i>	<i>p</i>
Arena	16	24.90	0.072
Genotype	1	0.87	0.352
Residual	50	81.97	—

895

896 Table S8. **List of candidate genes from LASSO of herbivore damage in the Zurich**
897 **site.** Estimated focal and neighbor genotype effects β_1 and β_2 are shown for non-zero
898 SNPs (see another file, *TableS_LASSOcandidate_HolesZurich.xlsx*).

899

900 Table S9. **Gene ontology (GO) enrichment analyses for candidate genes from**
901 **LASSO.** The GO terms were reduced using the REVIGO algorithm. The tab (A) and (B)
902 show the list of GO terms for candidate genes from positive and positive β_2 , respectively
903 (see another file, *TableS_LASSO_REVIGO.xlsx*).

904

905 References

- 906 1. L. Laikre, S. Hoban, M. W. Bruford, G. Segelbacher, F. W. Allendorf, G. Gajardo, A. G. Rodríguez, P. W. Hedrick, M. Heuertz, P. A. Hohenlohe, R. Jaffé, K. Johannesson, L. Liggins, A. J. MacDonald, P. OrozcoTerWengel, T. B. H. Reusch, H. Rodríguez-Correa, I.-R. M. Russo, N. Ryman, C. Vernesi, Post-2020 goals overlook genetic diversity. *Science*. **367**, 910 1083–1085 (2020).
- 911 2. M. Exposito-Alonso, T. R. Booker, L. Czech, L. Gillespie, S. Hateley, C. C. Kyriazis, P. L. M. Lang, L. Leventhal, D. Nogues-Bravo, V. Pagowski, M. Ruffley, J. P. Spence, S. E. Toro Arana, C. L. Weiß, E. Zess, Genetic diversity loss in the Anthropocene. *Science*. **377**, 914 1431–1435 (2022).
- 915 3. M. Stange, R. D. Barrett, A. P. Hendry, The importance of genomic variation for 916 biodiversity, ecosystems and people. *Nature Reviews Genetics*. **22**, 89–105 (2021).
- 917 4. T. G. Whitham, G. J. Allan, H. F. Cooper, S. M. Shuster, Intraspecific genetic 918 variation and species interactions contribute to community evolution. *Annual Review of 919 Ecology, Evolution, and Systematics*. **51**, 587–612 (2020).
- 920 5. B. Schmid, Effects of genetic diversity in experimental stands of *Solidago* 921 *altissima*—evidence for the potential role of pathogens as selective agents in plant 922 populations. *Journal of Ecology*, 165–175 (1994).
- 923 6. G. M. Crutsinger, M. D. Collins, J. A. Fordyce, Z. Gompert, C. C. Nice, N. J. Sanders, 924 Plant genotypic diversity predicts community structure and governs an ecosystem 925 process. *Science*. **313**, 966–968 (2006).
- 926 7. A. R. Hughes, B. D. Inouye, M. T. Johnson, N. Underwood, M. Vellend, Ecological 927 consequences of genetic diversity. *Ecology Letters*. **11**, 609–623 (2008).
- 928 8. S. Utsumi, Y. Ando, T. P. Craig, T. Ohgushi, Plant genotypic diversity increases 929 population size of a herbivorous insect. *Proceedings of the Royal Society B: Biological 930 Sciences*. **278**, 3108–3115 (2011).
- 931 9. J. Koriccheva, D. Hayes, The relative importance of plant intraspecific diversity in 932 structuring arthropod communities: A meta-analysis. *Functional Ecology*. **32**, 1704– 933 1717 (2018).
- 934 10. A. Raffard, F. Santoul, J. Cucherousset, S. Blanchet, The community and ecosystem 935 consequences of intraspecific diversity: A meta-analysis. *Biological Reviews*. **94**, 648– 936 661 (2019).
- 937 11. P. Barbosa, J. Hines, I. Kaplan, H. Martinson, A. Szczepaniec, Z. Szendrei, 938 Associational resistance and associational susceptibility: Having right or wrong 939 neighbors. *Annual Review of Ecology, Evolution, and Systematics*. **40**, 1–20 (2009).

- 940 12. Y. Sato, Associational effects and the maintenance of polymorphism in plant
941 defense against herbivores: Review and evidence. *Plant Species Biology*. **33**, 91–108
942 (2018).
- 943 13. H. Jactel, X. Moreira, B. Castagneyrol, Tree diversity and forest resistance to
944 insect pests: Patterns, mechanisms, and prospects. *Annual Review of Entomology*. **66**,
945 277–296 (2021).
- 946 14. P. A. Hambäck, B. D. Inouye, P. Andersson, N. Underwood, Effects of plant
947 neighborhoods on plant–herbivore interactions: Resource dilution and associational
948 effects. *Ecology*. **95**, 1370–1383 (2014).
- 949 15. M. C. Schuman, S. Allmann, I. T. Baldwin, Plant defense phenotypes determine the
950 consequences of volatile emission for individuals and neighbors. *eLife*. **4**, e04490
951 (2015).
- 952 16. K. G. Turner, C. M. Lorts, A. T. Haile, J. R. Lasky, Effects of genomic and functional
953 diversity on stand-level productivity and performance of non-native *Arabidopsis*.
954 *Proceedings of the Royal Society B*. **287**, 20202041 (2020).
- 955 17. S. E. Wuest, N. D. Pires, S. Luo, F. Vasseur, J. Messier, U. Grossniklaus, P. A.
956 Niklaus, Increasing plant group productivity through latent genetic variation for
957 cooperation. *PLoS Biology*. **20**, e3001842 (2022).
- 958 18. M. W. Horton, A. M. Hancock, Y. S. Huang, C. Toomajian, S. Atwell, A. Auton, N. W.
959 Mulyati, A. Platt, F. G. Sperone, B. J. Vilhjálmsdóttir, M. Nordborg, J. O. Borevitz, J.
960 Bergelson, Genome-wide patterns of genetic variation in worldwide *Arabidopsis*
961 *thaliana* accessions from the RegMap panel. *Nature Genetics*. **44**, 212–216 (2012).
- 962 19. C. Alonso-Blanco, J. Andrade, C. Becker, F. Bemm, J. Bergelson, K. M. Borgwardt, J.
963 Cao, E. Chae, T. M. Dezwaan, W. Ding, J. R. Ecker, M. Exposito-Alonso, A. Farlow, J. Fitz, X.
964 Gan, D. G. Grimm, A. M. Hancock, S. R. Henz, S. Holm, M. Horton, M. Jarsulic, R. A.
965 Kerstetter, A. Korte, P. Korte, C. Lanz, C.-R. Lee, D. Meng, T. P. Michael, R. Mott, N. W.
966 Mulyati, T. Nägele, M. Nagler, V. Nizhynska, M. Nordborg, P. Yu. Novikova, F. X. Picó, A.
967 Platzer, F. A. Rabanal, A. Rodriguez, B. A. Rowan, P. A. Salomé, K. J. Schmid, R. J. Schmitz,
968 U. Seren, F. G. Sperone, M. Sudkamp, H. Svardal, M. M. Tanzer, D. Todd, S. L.
969 Volchenboum, C. Wang, G. Wang, X. Wang, W. Weckwerth, D. Weigel, X. Zhou, 1,135
970 genomes reveal the global pattern of polymorphism in *Arabidopsis thaliana*. *Cell*. **166**,
971 481–491 (2016).
- 972 20. Y. Sato, E. Yamamoto, K. K. Shimizu, A. J. Nagano, Neighbor GWAS: Incorporating
973 neighbor genotypic identity into genome-wide association studies of field herbivory.
974 *Heredity*. **126**, 597–614 (2021).

- 975 21. Y. Sato, R. Shimizu-Inatsugi, M. Yamazaki, K. K. Shimizu, A. J. Nagano, Plant
976 trichomes and a single gene *GLABRA1* contribute to insect community composition on
977 field-grown *Arabidopsis thaliana*. *BMC Plant Biology*. **19**, 1–12 (2019).
- 978 22. B. Brachi, C. G. Meyer, R. Villoutreix, A. Platt, T. C. Morton, F. Roux, J. Bergelson,
979 Coselected genes determine adaptive variation in herbivore resistance throughout the
980 native range of *Arabidopsis thaliana*. *Proceedings of the National Academy of Sciences
981 USA*. **112**, 4032–4037 (2015).
- 982 23. Y. Sato, Y. Takahashi, C. Xu, K. K. Shimizu, Detecting frequency-dependent
983 selection through the effects of genotype similarity on fitness components. *Evolution*.
984 **77**, 1145–1157 (2023).
- 985 24. Y. Sato, H. Kudoh, Herbivore-mediated interaction promotes the maintenance of
986 trichome dimorphism through negative frequency-dependent selection. *The American
987 Naturalist*. **190**, E67–E77 (2017).
- 988 25. C. Gondro, J. H. Van Der Werf, B. Hayes, *Genome-wide association studies and
989 genomic prediction* (Humana Press, 2013).
- 990 26. R. Tibshirani, Regression shrinkage and selection via the lasso. *Journal of the
991 Royal Statistical Society: Series B (Methodological)*. **58**, 267–288 (1996).
- 992 27. S. Mochizuki, K. Sugimoto, T. Koeduka, K. Matsui, *Arabidopsis lipoxygenase 2* is
993 essential for formation of green leaf volatiles and five-carbon volatiles. *FEBS Letters*.
994 **590**, 1017–1027 (2016).
- 995 28. S. L. Zeller, O. Kalinina, D. F. Flynn, B. Schmid, Mixtures of genetically modified
996 wheat lines outperform monocultures. *Ecological Applications*. **22**, 1817–1826 (2012).
- 997 29. L.-N. Yang, Z.-C. Pan, W. Zhu, E.-J. Wu, D.-C. He, X. Yuan, Y.-Y. Qin, Y. Wang, R.-S.
998 Chen, P. H. Thrall, J. J. Burdon, L.-P. Shang, Q.-J. Sui, J. Zhan, Enhanced agricultural
999 sustainability through within-species diversification. *Nature Sustainability*. **2**, 46–52
1000 (2019).
- 1001 30. S. Atwell, Y. S. Huang, B. J. Vilhjalmsson, G. Willems, M. Horton, Y. Li, D. Meng, A.
1002 Platt, A. M. Tarone, T. T. Hu, R. Jiang, N. W. Muliyati, X. Zhang, M. A. Amer, I. Baxter, B.
1003 Brachi, J. Chory, C. Dean, M. Debieu, J. de Meaux, J. R. Ecker, N. Faure, J. M. Kniskern, J. D.
1004 G. Jones, T. Michael, A. Nemri, F. Roux, D. E. Salt, C. Tang, M. Todesco, M. B. Traw, D.
1005 Weigel, P. Marjoram, J. O. Borevitz, J. Bergelson, M. Nordborg, Genome-wide association
1006 study of 107 phenotypes in *Arabidopsis thaliana* inbred lines. *Nature*. **465**, 627–631
1007 (2010).
- 1008 31. M. W. Horton, N. Bodenhausen, K. Beilsmith, D. Meng, B. D. Muegge, S.
1009 Subramanian, M. M. Vetter, B. J. Vilhjálmsson, M. Nordborg, J. I. Gordon, J. Bergelson,
1010 Genome-wide association study of *Arabidopsis thaliana* leaf microbial community.
1011 *Nature Communications*. **5** (2014), doi:10.1038/ncomms6320.

- 1012 32. E. K. Chan, H. C. Rowe, D. J. Kliebenstein, Understanding the evolution of defense
1013 metabolites in *Arabidopsis thaliana* using genome-wide association mapping. *Genetics*.
1014 **185**, 991–1007 (2010).
- 1015 33. M. Togninalli, Ü. Seren, J. A. Freudenthal, J. G. Monroe, D. Meng, M. Nordborg, D.
1016 Weigel, K. Borgwardt, A. Korte, D. G. Grimm, AraPheno and the AraGWAS catalog 2020:
1017 A major database update including RNA-seq and knockout mutation data for
1018 *Arabidopsis thaliana*. *Nucleic Acids Research*. **48**, D1063–D1068 (2020).
- 1019 34. Y. Sato, R. Shimizu-Inatsugi, K. Takeda, B. Schmid, A. J. Nagano, K. K. Shimizu,
1020 *AraHerbNeighborGen: Arabidopsis herbivory data with the analysis of neighbor genotypic*
1021 *effects* (Zenodo, 2023; <https://doi.org/10.5281/zenodo.7945318>).
- 1022 35. J. Oksanen, F. G. Blanchet, M. Friendly, R. Kindt, P. Legendre, D. McGlinn, P. R.
1023 Minchin, R. B. O'Hara, G. L. Simpson, P. Solymos, M. H. H. Stevens, E. Szoecs, H. Wagner,
1024 *Vegan: Community ecology package* (2020; [https://CRAN.R-
1025 project.org/package=vegan](https://CRAN.R-project.org/package=vegan)).
- 1026 36. R Core Team, *R: A language and environment for statistical computing* (R
1027 Foundation for Statistical Computing, Vienna, Austria, 2019; [https://www.R-project.org/](https://www.R-
1028 project.org/)).
- 1029 37. K. A. Schneider, Maximization principles for frequency-dependent selection i:
1030 The one-locus two-allele case. *Theoretical Population Biology*. **74**, 251–262 (2008).
- 1031 38. H. Perdry, C. Dandine-Roulland, *Gaston: Genetic data handling (QC, GRM, LD, PCA)*
1032 *& linear mixed models* (2020; <https://CRAN.R-project.org/package=gaston>).
- 1033 39. T. Berardini, L. Reiser, E. Huala, TAIR functional annotation data (2021),
1034 doi:10.5281/zenodo.7159104.
- 1035 40. B. F. Voight, S. Kudaravalli, X. Wen, J. K. Pritchard, A map of recent positive
1036 selection in the human genome. *PLoS Biology*. **4**, e72 (2006).
- 1037 41. K. M. Siewert, B. F. Voight, Detecting long-term balancing selection using allele
1038 frequency correlation. *Molecular Biology and Evolution*. **34**, 2996–3005 (2017).
- 1039 42. M. Gautier, A. Klassmann, R. Vitalis, Rehh 2.0: A reimplementation of the R
1040 package rehh to detect positive selection from haplotype structure. *Molecular Ecology*
1041 *Resources*. **17**, 78–90 (2017).
- 1042 43. B. J. Balakumar, T. Hastie, J. Friedman, R. Tibshirani, N. Simon, *Glmnet for python*
1043 (2016; http://hastie.su.domains/glmnet_python/).
- 1044 44. Y. Benjamini, Y. Hochberg, Controlling the false discovery rate: A practical and
1045 powerful approach to multiple testing. *Journal of the Royal statistical society: series B*
1046 *(Methodological)*. **57**, 289–300 (1995).

- 1047 45. M. Carlson, *GO.db: A set of annotation maps describing the entire Gene Ontology*
1048 (2020; <https://doi.org/10.18129/B9.bioc.GO.db>).
- 1049 46. F. Supek, M. Bošnjak, N. Škunca, T. Šmuc, REVIGO summarizes and visualizes long
1050 lists of gene ontology terms. *PLoS One.* **6**, e21800 (2011).
- 1051 47. S. Sayols, *rrvgo: A bioconductor package to reduce and visualize gene ontology*
1052 *terms* (2020; <https://ssayols.github.io/rrvgo>).
- 1053 48. M. Carlson, *org.At.tair.db: Genome wide annotation for Arabidopsis* (2019;
1054 <https://doi.org/10.18129/B9.bioc.org.At.tair.db>).
- 1055 49. R. Kofler, C. Schlötterer, Gowinda: Unbiased analysis of gene set enrichment for
1056 genome-wide association studies. *Bioinformatics.* **28**, 2084–2085 (2012).
- 1057 50. Y. Sato, A. J. Nagano, *GOfisher* (Zenodo, 2023;
1058 <https://doi.org/10.5281/zenodo.7901509>).
- 1059 51. A. Kuznetsova, P. B. Brockhoff, R. H. B. Christensen, lmerTest package: Tests in
1060 linear mixed effects models. *Journal of Statistical Software.* **82**, 1–26 (2017).
- 1061 52. R. V. Lenth, *Emmeans: Estimated marginal means, aka least-squares means* (2021;
1062 <https://CRAN.R-project.org/package=emmeans>).
- 1063 53. D. Bates, M. Mächler, B. Bolker, S. Walker, Fitting linear mixed-effects models
1064 using lme4. *Journal of Statistical Software.* **67**, 1–48 (2015).
- 1065 54. Y. Sato, K. Takeda, A. J. Nagano, Neighbor QTL: An interval mapping method for
1066 quantitative trait loci underlying plant neighborhood effects. *G3; GenesGenomesGenetics.*
1067 **11**, jkab017 (2021).
- 1068 55. O. Folmer, M. Black, W. Hoeh, R. Lutz, R. Vrijenhoek, DNA primers for
1069 amplification of mitochondrial cytochrome c oxidase subunit I from diverse metazoan
1070 invertebrates. *Molecular Marine Biology and Biotechnology.* **3**, 294–299 (1994).
- 1071 56. L. Hendrich, J. Morinière, G. Haszprunar, P. D. N. Hebert, A. Hausmann, F. Köhler,
1072 M. Balke, A comprehensive barcode database for Central European beetles with a focus
1073 on Germany: Adding more than 3500 identified species to BOLD. *Molecular Ecology*
1074 *Resources.* **15**, 795–818 (2015).